NACA RM A57E02

NACA

RESEARCH MEMORANDUM

THE EFFECTS AT SUBSONIC SPEEDS OF WING FENCES AND A TAIL ON THE LONGITUDINAL CHARACTERISTICS OF A 63° SWEPT-WING AND FUSELAGE COMBINATION

By Donald A. Buell and Carl D. Kolbe

Ames Aeronautical Laboratory
Moffett Field, Calif.

NATIONAL ADVISORY COMMITTEE
FOR AERONAUTICS

WASHINGTON

July 2, 1957
Declassified September 1, 1959

NATIONAL ADVISORY COMMITTEE FOR AERONAUTICS

RESEARCH MEMORANDUM

THE EFFECTS AT SUBSONIC SPEEDS OF WING FENCES AND A TAIL ON THE LONGITUDINAL CHARACTERISTICS OF A 63° SWEPT-WING AND FUSELAGE COMBINATION

By Donald A. Buell and Carl D. Kolbe

SUMMARY

Wind-tunnel tests were made to evaluate the effects of wing fences and a tail on the longitudinal characteristics of a highly swept wing in combination with a fuselage. The model had a cambered and twisted wing with a leading-edge sweepback of 63° and an aspect ratio of 3.5. The model was tested with fences of various shapes and with both swept and unswept horizontal tails. The vertical and longitudinal positions and the incidence of the horizontal tail were varied. Results were obtained at Reynolds numbers of 3.5 million and 7 million at a Mach number of 0.20 and at Mach numbers of 0.60 to 0.95 at a Reynolds number of 2 million with angles of attack up to 22°.

The addition of six fences approximately twice as high as the maximum wing thickness and of a swept tail improved the static longitudinal stability to a limited degree. For the model so equipped, the loss in static margin at low speeds as determined by tests at 0.20 Mach number was about 12 percent in the interval from a lift coefficient of 0 to 0.8. A breakdown of the factors affecting stability showed that at low speeds large tail volumes were desirable and that the fences had either a small or adverse effect on the flow at the tail. The addition of the fences and of the tail each decreased the maximum lift-drag ratio for the trimmed condition by the order of 15 percent.

INTRODUCTION

It has been previously demonstrated that a thin highly swept wing is capable of large lift-drag ratios at speeds well into the supersonic regime. Reference 1 reports lift-drag ratios of 9 at a Mach number of 1.5 for one such wing-body combination in which the wing had a thickness-chord

ratio of 0.05, a leading-edge sweepback of 63°, and an aspect ratio of 3.5. This lift-drag ratio was achieved despite the lack of body indentation, which has since been shown to be beneficial (see ref. 2, for example). This wing has a disadvantage that is typical of a wide range of plan forms with high sweep: The static longitudinal stability decreases abruptly at some moderate lift coefficient. References 3 and 4 showed that a model geometrically similar to that of reference 1 had this unfavorable stability characteristic at all subsonic speeds. Reference 5 discusses the phenomenon and concludes that it is a result of leading-edge flow separation. One method of delaying the separation is to provide camber and twist in the wing; these improvements were already incorporated in the wings of references 1, 3, and 4. There are also certain devices, such as wing fences, to control the spanwise location of the separation so as to improve the pitching-moment characteristics of highly swept wings. Reference 6 describes the partially successful results of using such devices. A third method of improving stability characteristics is to place a horizontal tail in the downwash field of the wing so that it provides increases in stability at the angle of attack where the wing loses stability.

The purpose of the present investigation was to use all three methods of improving the longitudinal stability of a thin highly swept wing and to assess the resulting lift and drag penalties. For this purpose a model configuration similar to that of reference 1 was tested in the Ames 12-foot pressure wind tunnel at Mach numbers from 0.20 to 0.95 and at Reynolds numbers from 2 million to 7 million. The test data are reported herein.

NOTATION

a_t lift-curve slope of the isolated horizontal tail

a_w lift-curve slope of the wing-fuselage combination

b wing span

C_D drag coefficient, $\frac{\text{drag}}{qS}$

C_L lift coefficient, $\frac{\text{lift}}{qS}$

C_m pitching-moment coefficient, $\frac{\text{pitching moment}}{qS\bar{c}}$

C_{m_t} pitching-moment coefficient due to the tail, $\frac{C_{m_{\text{tail on}}} - C_{m_{\text{tail off}}}}{qS\bar{c}}$

c	wing chord measured parallel to the plane of symmetry
$\bar{c}$	wing mean aerodynamic chord
i_t	incidence of the horizontal tail
l_t	tail length, longitudinal distance from the moment center to the pivot line of the horizontal tail
$\frac{L}{D}$	lift-drag ratio
M	free-stream Mach number
q	free-stream dynamic pressure
q_t	effective dynamic pressure at the horizontal tail
R	Reynolds number, based on wing mean aerodynamic chord
S	wing area
S_t	horizontal-tail area
V	horizontal-tail volume, $\frac{l_t}{\bar{c}} \frac{S_t}{S}$
α	angle of attack of the fuselage center line
α_t	effective angle of attack of the horizontal tail
ϵ	effective angle of downwash at the horizontal tail
η	tail efficiency factor

Subscripts

trimmed	$C_m = 0$
w	wing-fuselage combination

MODEL AND APPARATUS

Photographs of the model are presented in figure 1, and the dimensions are given in figure 2 and in table I. The wing, which had previously been used in the investigations of references 3 and 4, had a leading-edge sweep of 63°, an aspect ratio 3.5, and a taper ratio of 0.25. The streamwise airfoil sections were NACA 64A005 combined with a = 1 camber lines. Figure 3 shows the spanwise distribution of camber and twist. For the present investigation the elevons were not deflected, and the gap between wing and elevons was filled. The body was constructed to permit installation of the wing on the body in either a mid or high position. All parts of the model, except the fences, were constructed of steel. The model was mounted on a four-component strain-gage balance enclosed by the model body, and the balance was supported by a 4-inch-diameter sting.

Two horizontal tails were used, one unswept (as measured at the mid-chord line in this particular case) and the other swept back 60° at the leading edge. Either could be mounted on the body at the center line. The unswept tail could also be mounted above the body on the vertical tail. It was also possible to position the tail assembly in either of two longitudinal positions. This was accomplished by the insertion of cylindrical sections of different lengths in the maximum-diameter portion of the body.

Fences were made from 0.051-inch brass sheet in the shapes shown in figure 4. Fences I to IX were equipped with 1/2-inch flanges on the inboard side and could be screwed to the wing at stations 0.30, 0.50, or 0.75 b/2 from the plane of symmetry. Fence X was soldered directly to the wing at stations 0.29, 0.45, and 0.70 b/2 from the plane of symmetry. Fences II through IX were constructed by attaching a piece of the desired shape to the fence I structure and removing unwanted portions and thus were of double thickness on certain parts of the fence.

TESTS

Initial tests were exploratory in nature, consisting of static force and moment measurements with many configuration changes. These measurements were made mainly at low speeds, and the improvement of the pitching-moment characteristics was the primary concern. On the basis of these tests, a model configuration was selected which was considered suitable for a more complete investigation. In this configuration the swept horizontal tail was used, and the wing was mounted in a mid position on the fuselage and had six fences (three on each wing panel) of the shape designated as fence X (see fig. 4).

Static force and moment measurements were made of the selected configuration which would show the effects of tail length, tail incidence, Mach number, and Reynolds number. Tests with the fences off and tail off were also made for comparison. The angle of attack was varied from -4° to about 22° except where model strength or choking of the tunnel flow limited the range to lower values. The model was tested at Mach numbers up to 0.95 at a Reynolds number of 2 million and at Reynolds numbers up to 7 million at a Mach number of 0.20.

CORRECTIONS TO DATA

The data were corrected for the induced effects of the tunnel walls resulting from lift on the model by the method of reference 7. The corrections were as follows:

$$\Delta\alpha = 0.30\ C_L$$

$$\Delta C_D = 0.0045\ C_L^2$$

$$\Delta C_m = 0.003\ C_L$$

The data were corrected for the constriction effects of the tunnel walls by the method of reference 8. This correction amounted to less than 2 percent of the Mach number and dynamic pressure at the highest test Mach number.

The pressure at the base of the model was measured, and the drag data were adjusted to correspond to a base pressure equal to free-stream static pressure. This procedure provided a partial compensation for the interference between the model and the sting, and for a static-pressure gradient in the tunnel air stream near the rear of the model. The largest pressure gradient was encountered with the extended-body configurations at Mach numbers near 0.90, for which the static pressure at the station of the horizontal tail was higher than that of the free stream by about 3 percent of the free-stream dynamic pressure. No correction was applied to the lift or pitching-moment data for these effects.

RESULTS AND DISCUSSION

The primary aim of this investigation was to obtain as nearly as possible a linear variation of pitching moment with lift. The discussion will deal first with the configuration changes which were explored in an attempt to improve the pitching-moment characteristics. Results of tests

on the final configuration selected will then be presented together with an analysis of these results. In order to provide a realistic basis for evaluating the results, the center of moments was changed with each modification to the model so as to maintain approximately the same static margin at low lift coefficients. The centers of moments are given in table II, along with the corresponding tail lengths and tail volumes.

Exploratory Tests

Figure 5 shows some of the results obtained from initial low-speed tests. The comparisons are intended to be only qualitative because the effects of many variables such as Mach number and Reynolds number were not isolated except where it was expeditious to do so. The pitching-moment characteristics of the model without horizontal tail or fences is represented by the dashed line in figure 5. The addition of fences by themselves was effective for only a small range of lift coefficients. The addition of the tail with no fences supplied a favorable increment to the slope of the pitching-moment curve at high lift coefficients and also at moderate lift coefficients when mounted in a mid position. The largest range of lift coefficients for which the model was stable was obtained with a combination having six wing fences, twice as high as the maximum wing thickness, and a tail. The effects of reducing the fence height near the wing leading edge or even of eliminating the forward part of the fence were small. Reducing the over-all fence height or, particularly, the height near the quarter-chord point caused large losses in effectiveness. Tests with the fences at various spanwise locations showed that the inboard fences were much more effective than the outboard fences, though all evidently contributed to the stability improvement. The effects of wing height and tail sweep on stability were small.

Quantitative results for two configurations are shown in figure 6. It can be seen that the addition of six fences twice as high as the maximum wing thickness and of an unswept horizontal tail caused the lift coefficient for $dC_m/dC_L = 0$ to be increased from 0.5 to 0.9. It can also be seen that the drag has been greatly increased at low lift coefficients. The selection of a final configuration was then guided by the desire to reduce drag at high speeds without forfeiting the improvement in the low-speed pitching-moment characteristics. To this end the fence height at the leading edge of the wing was reduced, and the fence attaching flanges were eliminated by soldering the fences to the wing. At high speeds the measured drags were lowest for the mid-wing and swept-tail combination; therefore these features were also included in the final configuration.

Final-Configuration Tests

Figures 7, 8, and 9 show the longitudinal characteristics of the model having a mid wing, a swept horizontal tail, and six fences of the shape designated as fence X. Data are presented for two tail lengths, four tail incidences from 0.2° to -11.7°, and the tail-off condition. It should be noted that only the tail-off configurations have the same moment center for all three combinations of fences and body lengths.

The best pitching-moment characteristics at high lifts and low speeds were obtained with the model having fences and the longer tail length. Figure 7 shows that even this configuration was almost neutrally stable when trimmed at a lift coefficient of 0.8. The loss in static margin was about 12 percent in the interval from $C_L = 0$ to $C_L = 0.8$ (model trimmed). Neither the tail nor the fences eliminated the rather abrupt increase in stability which occurred at all Mach numbers with increasing lift coefficients near 0.2 to 0.4. In addition, the fences increased the unstable variation of pitching moment, which occurred at the higher lift coefficients at most Mach numbers. Increasing Mach number caused some increases in static margin at the higher lift coefficients for all configurations but was particularly beneficial to the configurations without fences.

The lift curves of figure 8 show that the fences produced very little net change in lift coefficient for most angles of attack despite their sometimes large effect on the pitching moment. At high angles of attack the lift decrements due to the fences became large, especially at high Mach numbers.

Losses in maximum lift-drag ratio due to the fences (fig. 9(a)) were between approximately 15 and 20 percent. The large magnitude of this loss is due in part to the flow separation which existed inboard of each fence. It is of interest to compare the decrements of lift-drag ratio due to fences with the much smaller decrements due to lengthening the fuselage and to note that both modifications increased the wetted area of the model by approximately equal amounts. The increase in minimum-drag coefficient of the model due to the fences varied from about 0.003 to 0.004, being least at the highest Reynolds number and the lowest Mach number. The elimination of the attaching flanges, which were used in the exploratory tests to secure the fences to the wing, decreased the minimum-drag coefficient by about 0.001 at the highest Reynolds number.

For the centers of moments selected, the tail load required to trim the model was quite small in the region of maximum lift-drag ratios, and the associated tail drag was also small. At a tail incidence of -3.9°, for which the model was approximately trimmed, the maximum lift-drag ratio was reduced about 5 or 10 percent by the addition of a horizontal and vertical tail. It may be noted that the exposed surface area of the empennage was almost twice that of the fences.

Summary of Static Longitudinal Stability Factors

Figure 10 presents a summary of the stability of the final configuration for a low- and a high-speed condition and a breakdown of the more important components of stability. In this figure the stability is represented by the slope of the pitching-moment curve, dC_m/dC_L, for the tail incidence at which the model was trimmed. This value was obtained from cross plots and is only approximate because the nonlinear tail-lift characteristics caused the tail contribution to stability to be nonlinear with tail incidence. The parameters presented in figure 10 have the following approximate relation:

$$\left(\frac{dC_m}{dC_L}\right)_{trimmed} \approx \left(\frac{dC_m}{dC_L}\right)_w - V\frac{a_t}{a_w}\left(1 - \frac{d\epsilon}{d\alpha}\right)\eta\frac{q_t}{q}$$

The value of a_t was estimated to be 0.043 per degree. The factors $1-(d\epsilon/d\alpha)$ and $\eta(q_t/q)$ were determined from the data using the following relations:

$$1 - (d\epsilon/d\alpha) = (\partial\alpha_t/\partial\alpha)_{i_t = \text{constant}}$$

$$\alpha_t = \frac{C_{m_t}}{(\partial C_m/\partial i_t)_{\alpha = \text{constant}}}$$

$$\eta(q_t/q) = -[1/(a_t V)](\partial C_m/\partial i_t)_{\alpha = \text{constant}}$$

When nonlinearities in the data make the determination of these factors questionable, the values are not shown.

The curves of dC_m/dC_L in figure 10(a) illustrate the stability increases resulting from the longer tail length and from the fences at the higher lift coefficients. The curves of $1 - (d\epsilon/d\alpha)$ and $\eta(q_t/q)$ show that the downwash and wake characteristics were practically unaffected by changing the tail length. The superiority of the longer tail length at low speeds was due to the fact that the tail contribution to stability generally increased with lift, making a large tail volume more desirable. The fences also had little effect on the downwash and wake characteristics at low speeds for trimmed lift coefficients up to 0.7. The curves of dC_m/dC_L show that above this lift coefficient the stability

afforded by the fences was greatly reduced by the presence of the tail, presumably because of adverse effects on the downwash or wake fields.

At a Mach number of 0.90 (fig. 10(b)) the fences were not as effective on the wing-body combination as they were at low speeds. However, by virtue of their favorable influence on the downwash field and on the ratio of tail to wing lift-curve slopes, they were beneficial to the stability of the complete model at lift coefficients up to 0.6.

Maximum Lift-Drag Ratios

Figure 11 presents the maximum lift-drag ratios and the corresponding lift coefficients of the model in a trimmed condition, as determined from cross plots of the data. Lift-drag ratios of the final configuration with and without fences are compared to those of the model of reference 4 which used elevons for trimming. Losses due to the use of a tail were of the order of 15 percent, as were those due to fences. However, the tail effect included losses due to the vertical tail as well as the horizontal tail, to the lengthened fuselage, and to elevon influences which were less favorable in the undeflected condition than in the trimmed condition.

The minimum drag coefficients of the various model configurations are also presented in figure 11. Calculations at a given lift coefficient indicate that the increments in minimum drag coefficient due to the addition of tail and fences accounts for at least three-fourths of the losses in maximum lift-drag ratio that are shown. A conclusion of reference 1 was that the effects of Mach number on maximum lift-drag ratio in the supersonic regime were also primarily due to changes in minimum drag coefficient, resulting from changes in thickness drag. It seems likely that the reduction in lift-drag ratio at the design Mach number of 1.5 due to addition of the tail would be roughly the same percentage as at subsonic Mach numbers.

SUMMARY OF RESULTS

The effects of wing fences and of a tail on the longitudinal characteristics of the model have been evaluated for subsonic speeds. The model had a cambered and twisted wing with a leading-edge sweepback of 63° and an aspect ratio of 3.5. For the configuration employing six fences approximately twice as high as the maximum wing thickness, mid-wing mounting, and a swept tail, the following results were obtained:

1. The addition of the fences and tail improved the static longitudinal stability to a limited degree. At low speeds the loss in static margin for the model in the trimmed condition was about 12 percent in the

interval from a lift coefficient of 0 to 0.8. The fences and tail did not eliminate the abrupt increase in stability at moderate lifts, and the fences increased the unstable variation of pitching moment at the highest lifts.

2. A breakdown of the factors affecting stability showed that at low speeds the effective downwash and wake characteristics were practically unaffected by a change in tail length. However, the tail contribution to stability generally increased with lift coefficient, making a large tail volume desirable. The effect of the fences on the downwash and wake characteristics at low speeds was either small or adverse.

3. The addition of the fences and of the tail to the basic elevon-controlled configuration each decreased the maximum lift-drag ratio for the trimmed condition by the order of 15 percent.

Ames Aeronautical Laboratory
National Advisory Committee for Aeronautics
Moffett Field, Calif., May 2, 1957

REFERENCES

1. Hall, Charles F., and Heitmeyer, John C.: Aerodynamic Study of a Wing-Fuselage Combination Employing a Wing Swept Back 63°. - Characteristics at Supersonic Speeds of a Model With the Wing Twisted and Cambered for Uniform Load. NACA RM A9J24, 1950.

2. Sevier, John R., Jr.: Investigation of the Effects of Body Indentation and of Wing-Plan-Form Modification on the Longitudinal Characteristics of a 60° Swept-Wing-Body Combination at Mach Numbers of 1.41, 1.61, and 2.01. NACA RM L55E17, 1955.

3. Jones, J. Lloyd, and Demele, Fred A.: Aerodynamic Study of a Wing-Fuselage Combination Employing a Wing Swept Back 63°. - Characteristics Throughout the Subsonic Speed Range With the Wing Cambered and Twisted for a Uniform Load at a Lift Coefficient of 0.25. NACA RM A9D25, 1949.

4. Jones, J. Lloyd, and Demele, Fred A.: Aerodynamic Study of a Wing-Fuselage Combination Employing a Wing Swept Back 63°. - Effects at Subsonic Speeds of a Constant-Chord Elevon on a Wing Cambered and Twisted for a Uniform Load at a Lift Coefficient of 0.25. NACA RM A9I27, 1949.

5. Furlong, G. Chester, and McHugh, James G.: A Summary and Analysis of the Low-Speed Longitudinal Characteristics of Swept Wings at High Reynolds Number. NACA RM L52D16, 1952.

6. Fischetti, Thomas L.: Effects of Fences, Leading-Edge Chord Extensions, Boundary-Layer Ramps, and Trailing-Edge Flaps on the Longitudinal Stability of a Twisted and Cambered 60° Sweptback-Wing - Indented-Body Configuration at Transonic Speeds. NACA RM L54D09a, 1954.

7. Sivells, James C., and Salmi, Rachel M.: Jet-Boundary Corrections for Complete and Semispan Swept Wings in Closed Circular Wind Tunnels. NACA TN 2454, 1951.

8. Herriot, John G.: Blockage Corrections for Three-Dimensional-Flow Closed-Throat Wind Tunnels, With Consideration of the Effects of Compressibility. NACA Rep. 995, 1950. (Formerly NACA RM A7B28)

TABLE I.- GEOMETRIC PROPERTIES OF THE MODEL

Wing	
Area, sq ft	4.02
Aspect ratio	3.50
Span, ft	3.75
Taper ratio	0.25
Mean aerodynamic chord, ft	1.20
Sweepback (leading edge), deg	63.0
Section (streamwise)	NACA 64A005
Incidence (at plane of symmetry), deg	0
Horizontal tails	
Swept tail	
Area, sq ft	1.00
Aspect ratio	2.50
Span, ft	1.58
Taper ratio	0.20
Sweepback (leading edge), deg	60.0
Section (streamwise)	NACA 0004-64
Pivot axis (fraction of root chord)	0.84
Unswept tail	
Area, sq ft	0.87
Aspect ratio	4.00
Span, ft	1.87
Taper ratio	0.33
Sweepback of 50-percent chord line, deg	0
Section	NACA 0004-64
Pivot axis (fraction of root chord)	0.45
Vertical tail (leading and trailing edges extended to fuselage center line)	
Area, sq ft	1.07
Aspect ratio	1.51
Span, ft	1.27
Taper ratio	0.16
Sweepback (leading edge), deg	54.0
Section (streamwise)	NACA 0003.5-64
Fuselage	
Fineness ratio	
Short fuselage	12.00
Long fuselage	13.75
Base area, sq ft	0.13

TABLE I.- GEOMETRIC PROPERTIES OF THE MODEL - Concluded

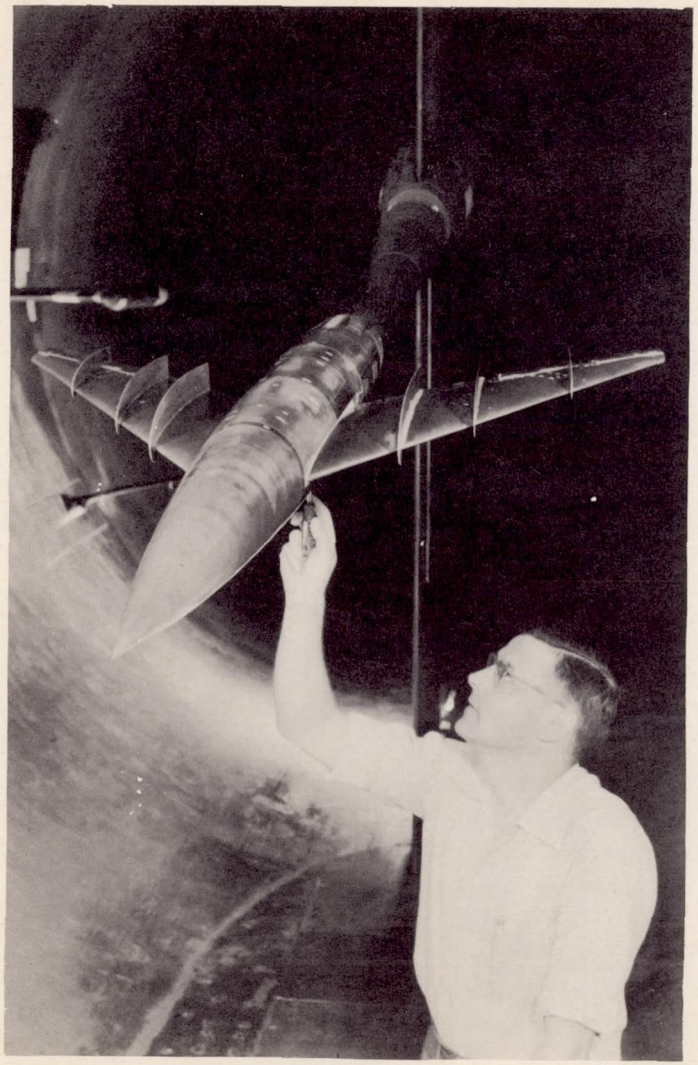
Coordinates[1] (long fuselage):

Distance from nose, inches	Radius, inches
0	0
5.00	.80
10.00	1.44
15.00	1.94
20.00	2.32
25.00	2.60
30.00	2.79
35.00	2.90
40.00	2.97
45.25	2.99
51.25	3.00
68.25	3.00
72.25	2.99
76.25	2.90
80.25	2.67
82.50	2.44

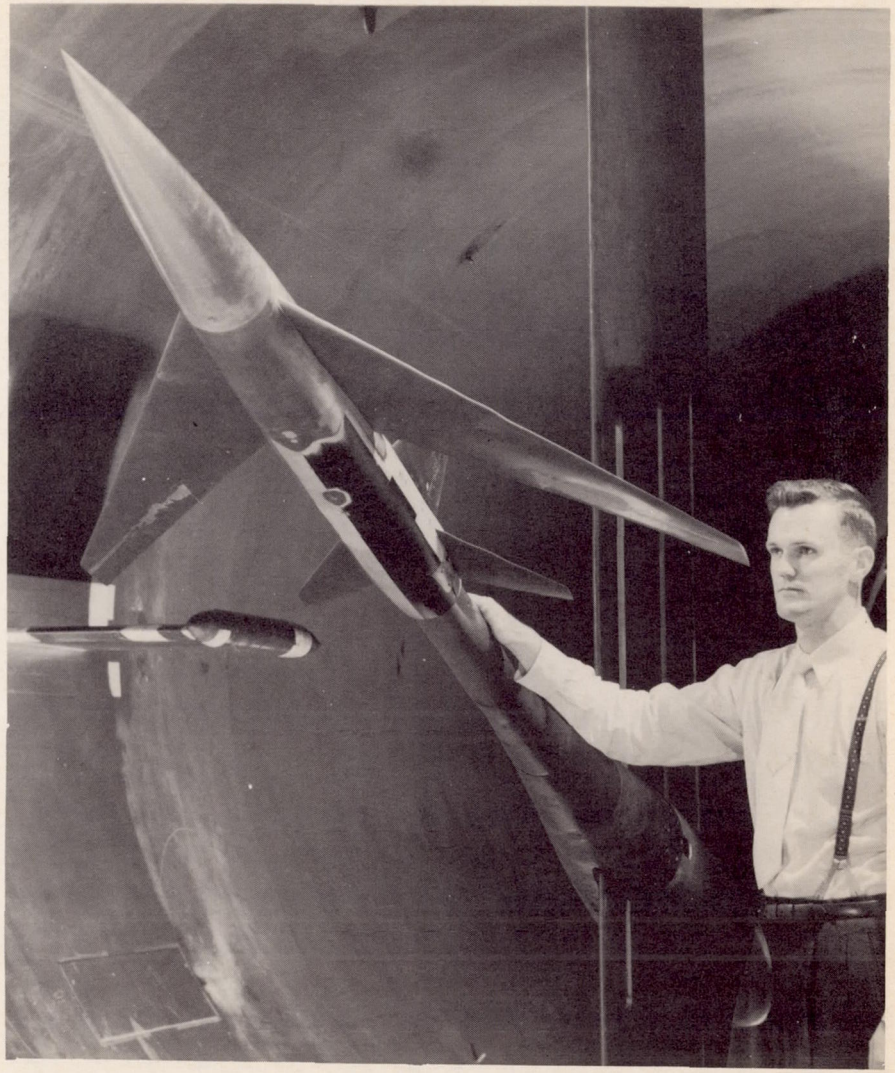
[1]Removable section from 51.25 to 68.25 inches from nose.

TABLE II.- MOMENTS CENTERS, TAIL LENGTHS, AND TAIL VOLUMES

Configuration			Moment center, $\frac{\overline{c}}{c}$	Tail length, $l_t/\overline{c}$	Tail volume, V
Fuselage	Tail	Fences			
Short or long	Off	On or off	0.25	---	---
Short	Unswept	On	.40	1.52	0.331
Short	Swept	On	.40	1.52	.380
Long	Swept	On	.45	2.20	.549
Long	Swept	Off	.50	2.16	.538



A-20846



A-19828

Figure 1.- Model mounted in the wind tunnel.

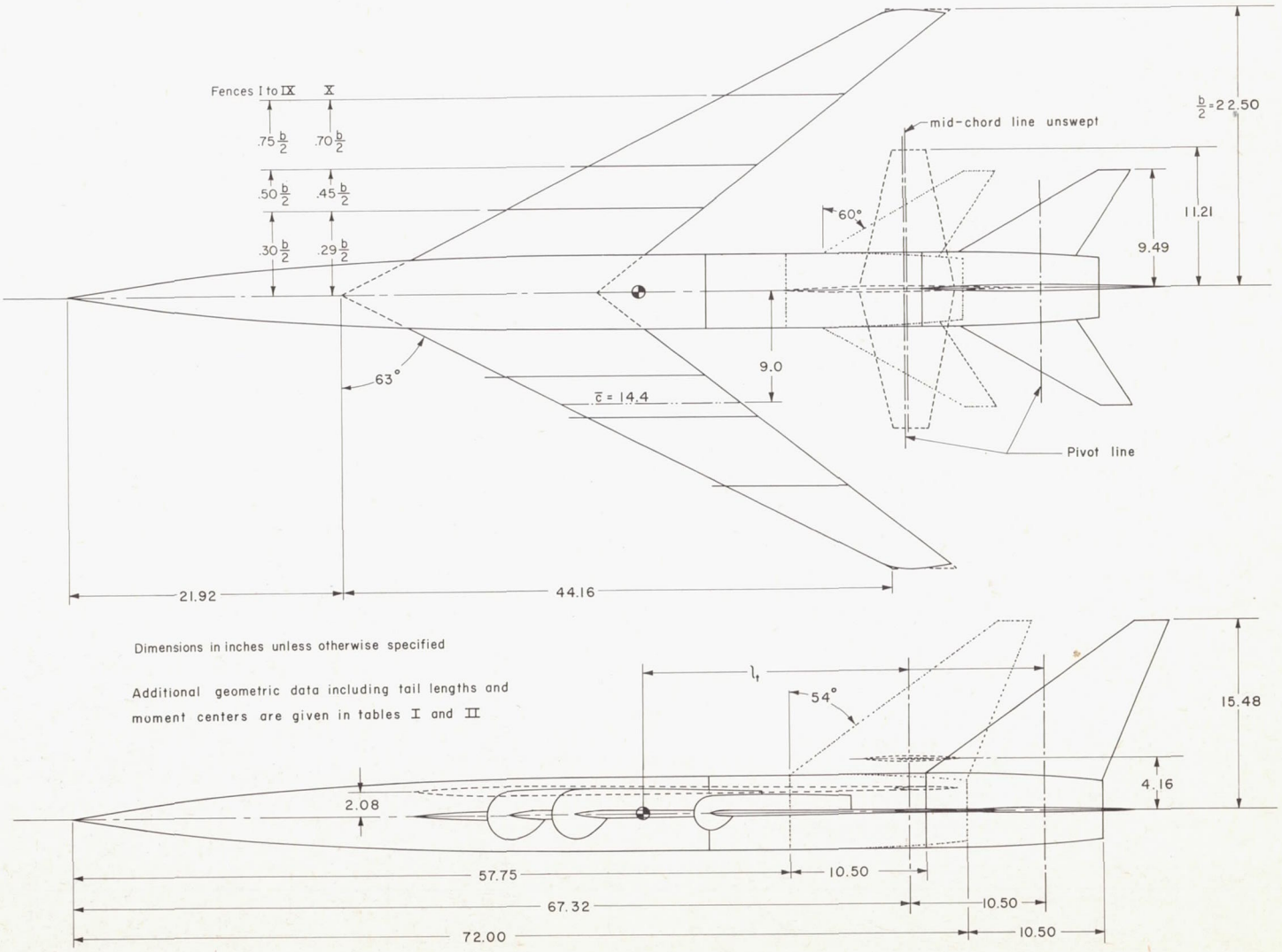


Figure 2.- Geometry of the model.

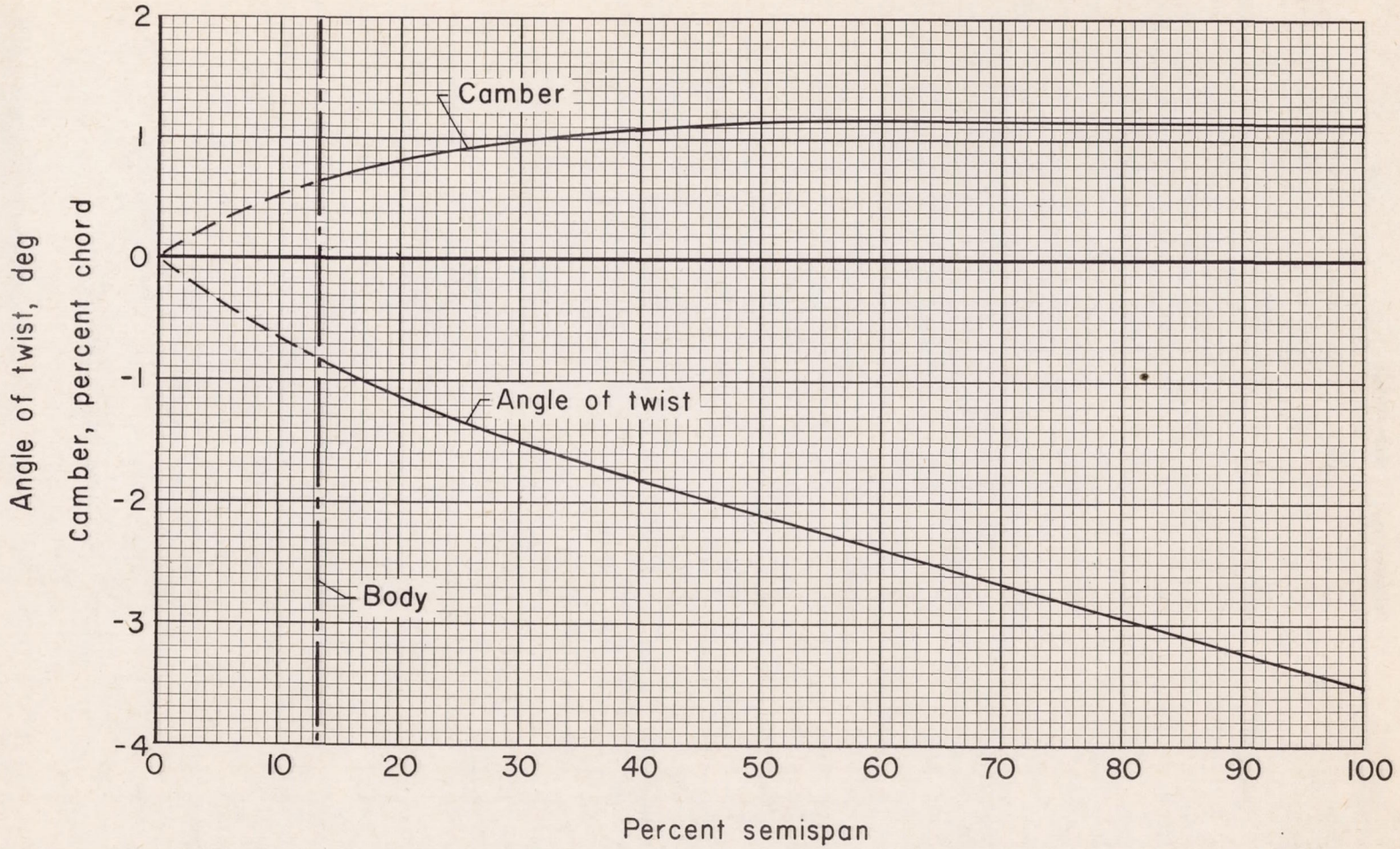


Figure 3.- Mean camber and twist of the wing.

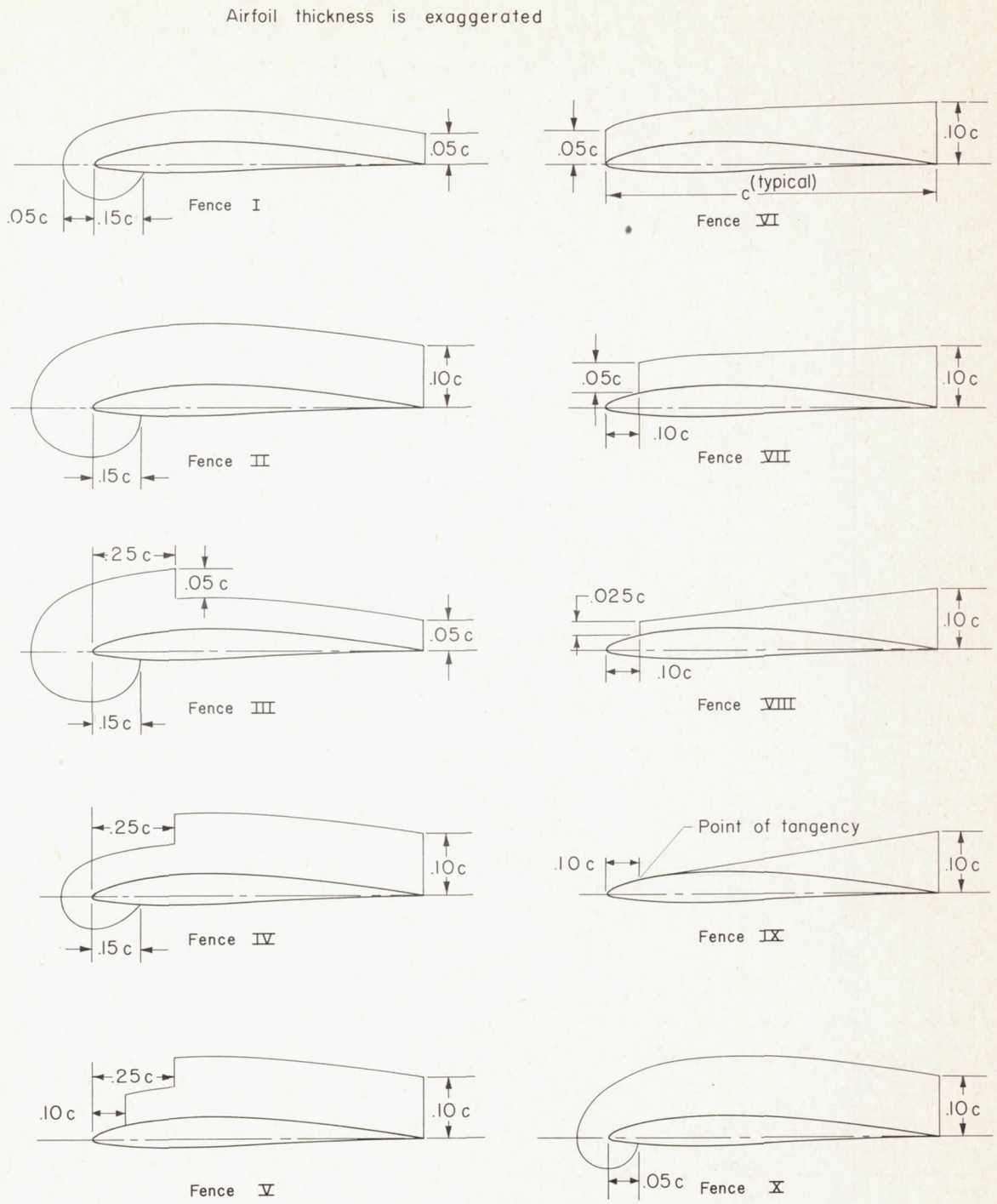


Figure 4.- Fence profiles.

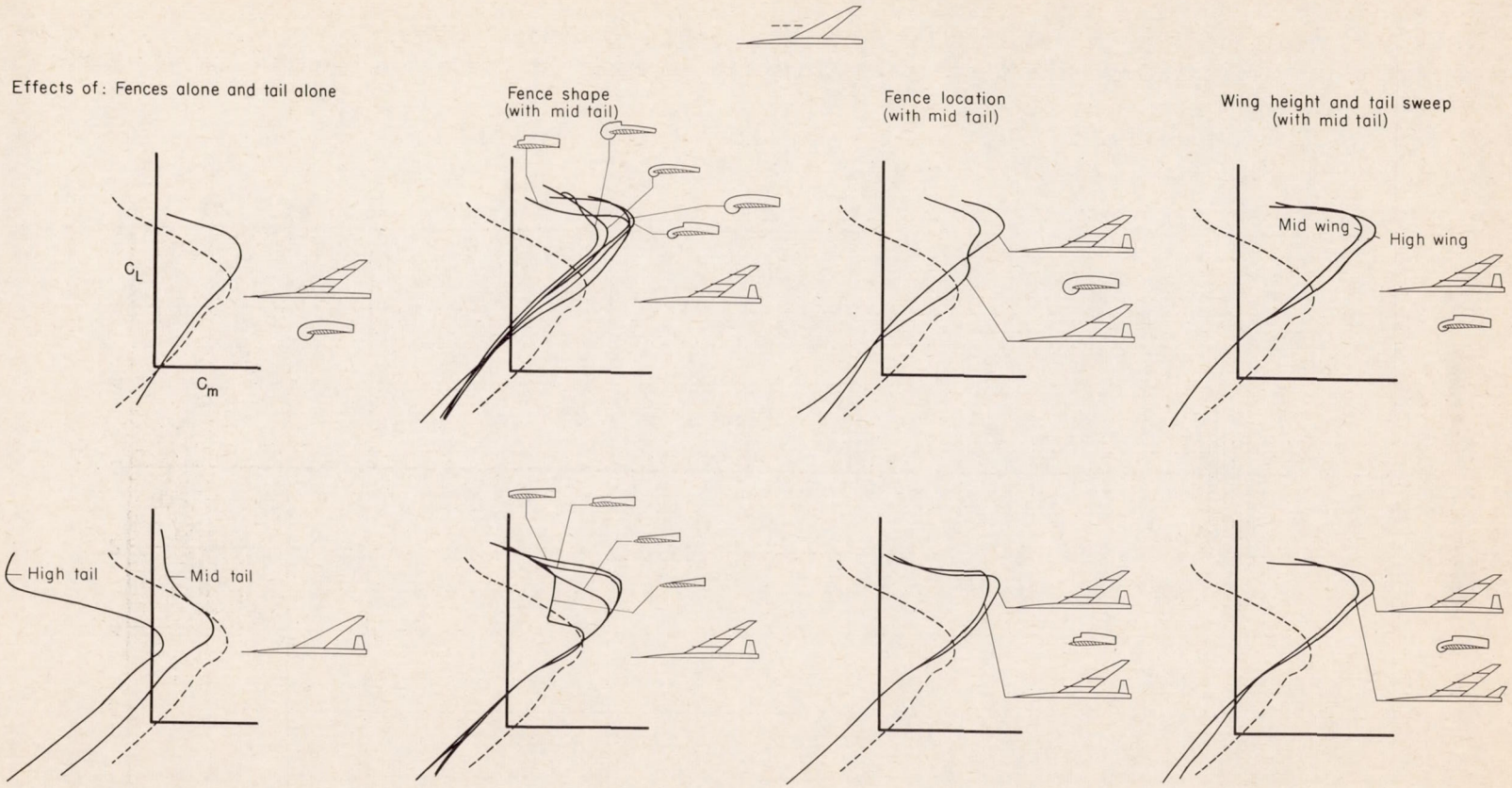


Figure 5.- The effects of changes in model configuration on the pitching-moment characteristics of the model at low speed.

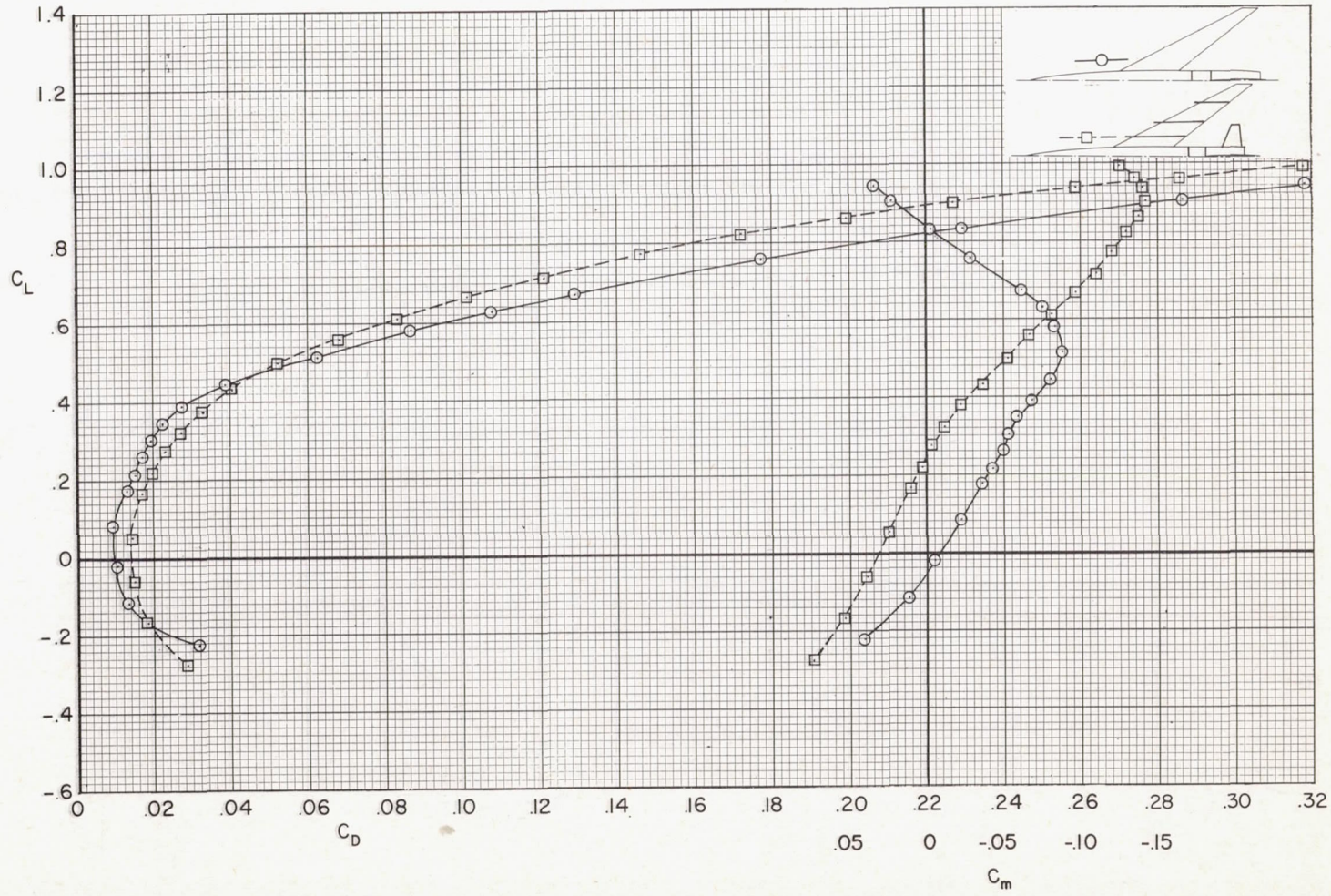
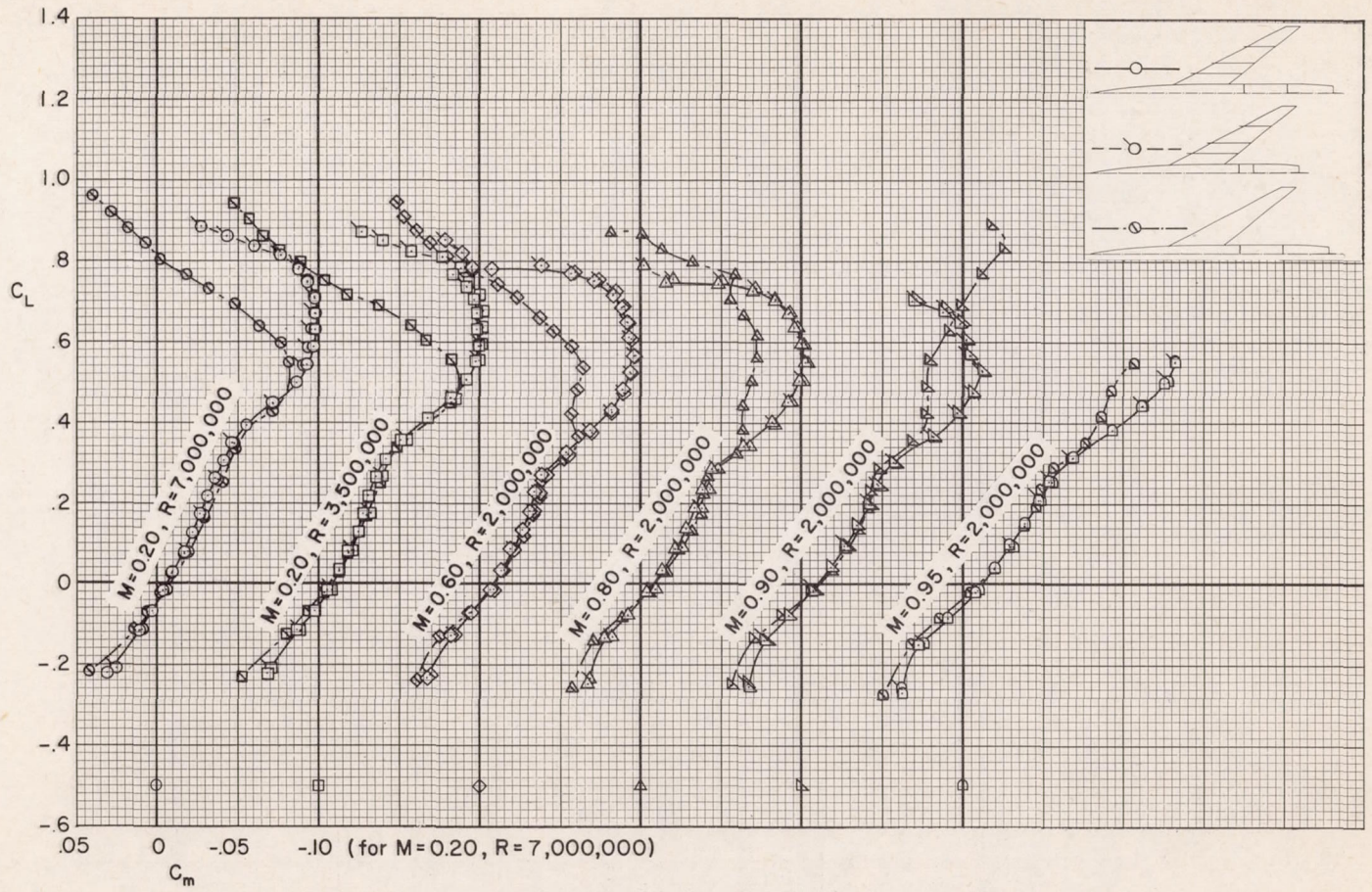
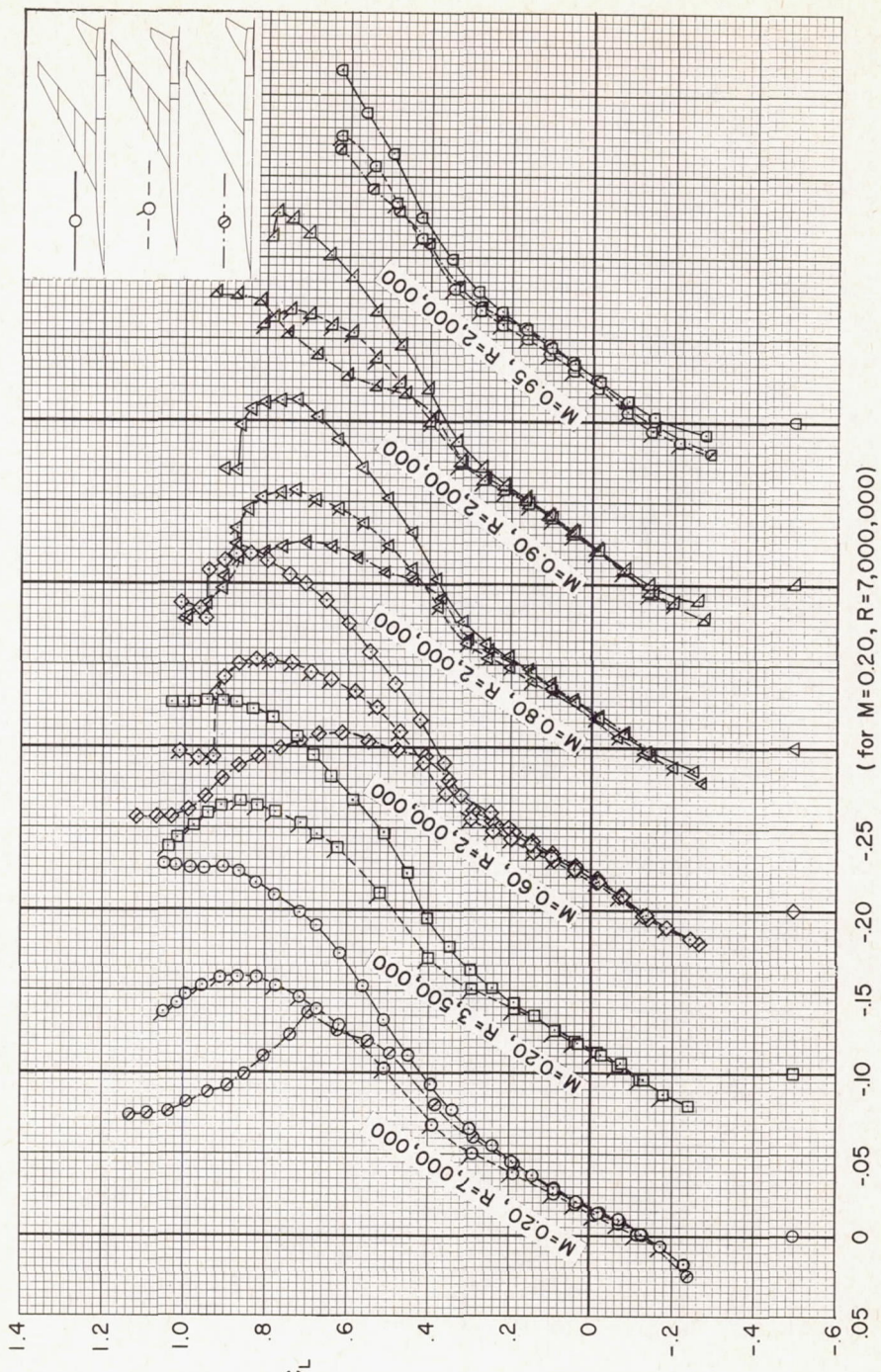


Figure 6.- The effects of fences and tail on the drag and pitching-moment characteristics of the model; M = 0.20, R = 7,000,000, fence configuration II, wing and tail in mid position, $i_t = -3.9^\circ$.



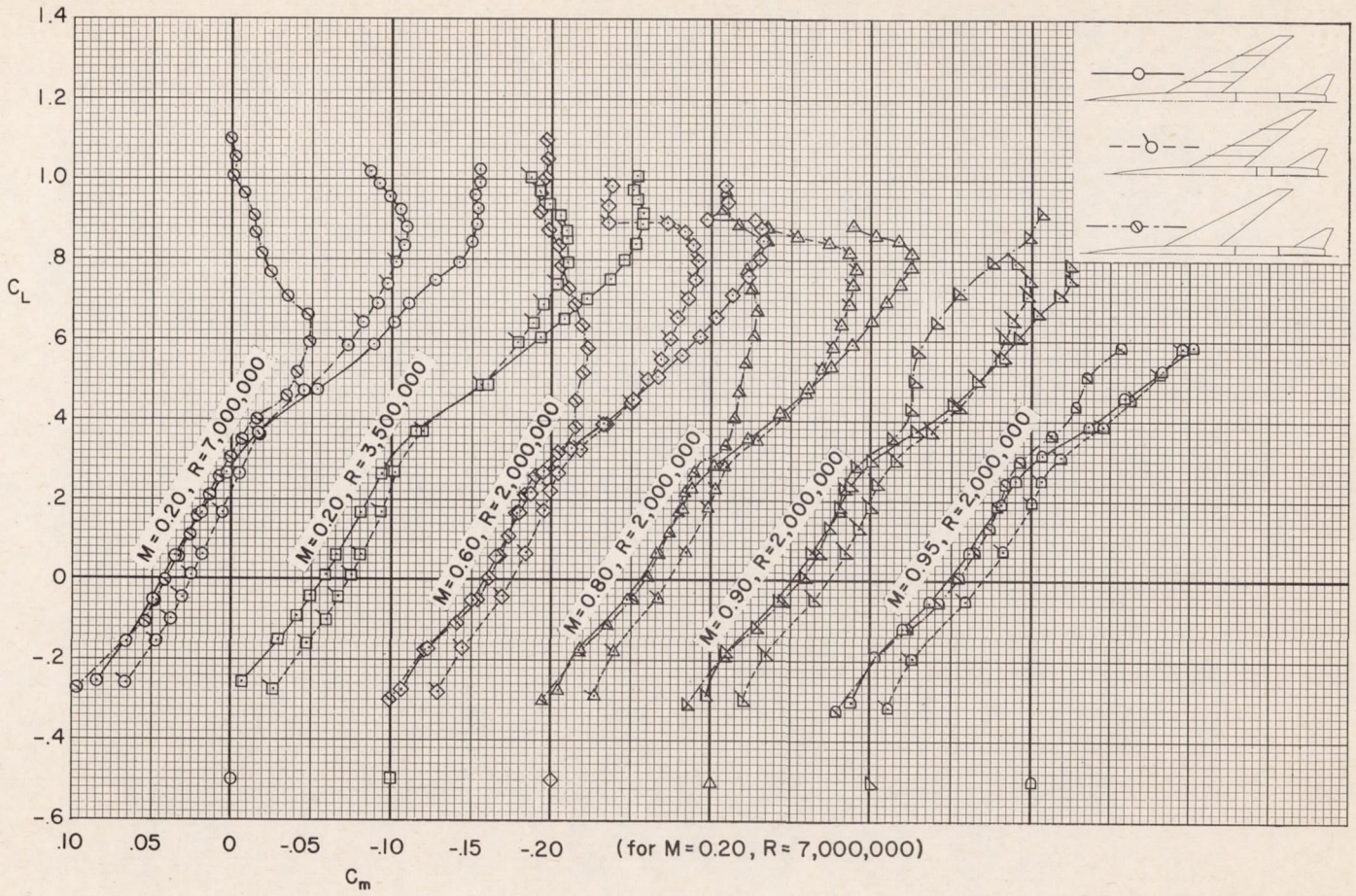
(a) Tail off.

Figure 7.- The pitching-moment characteristics of the model; wing in mid position, with and without fences (configuration X) and empennage (horizontal tail in mid position).



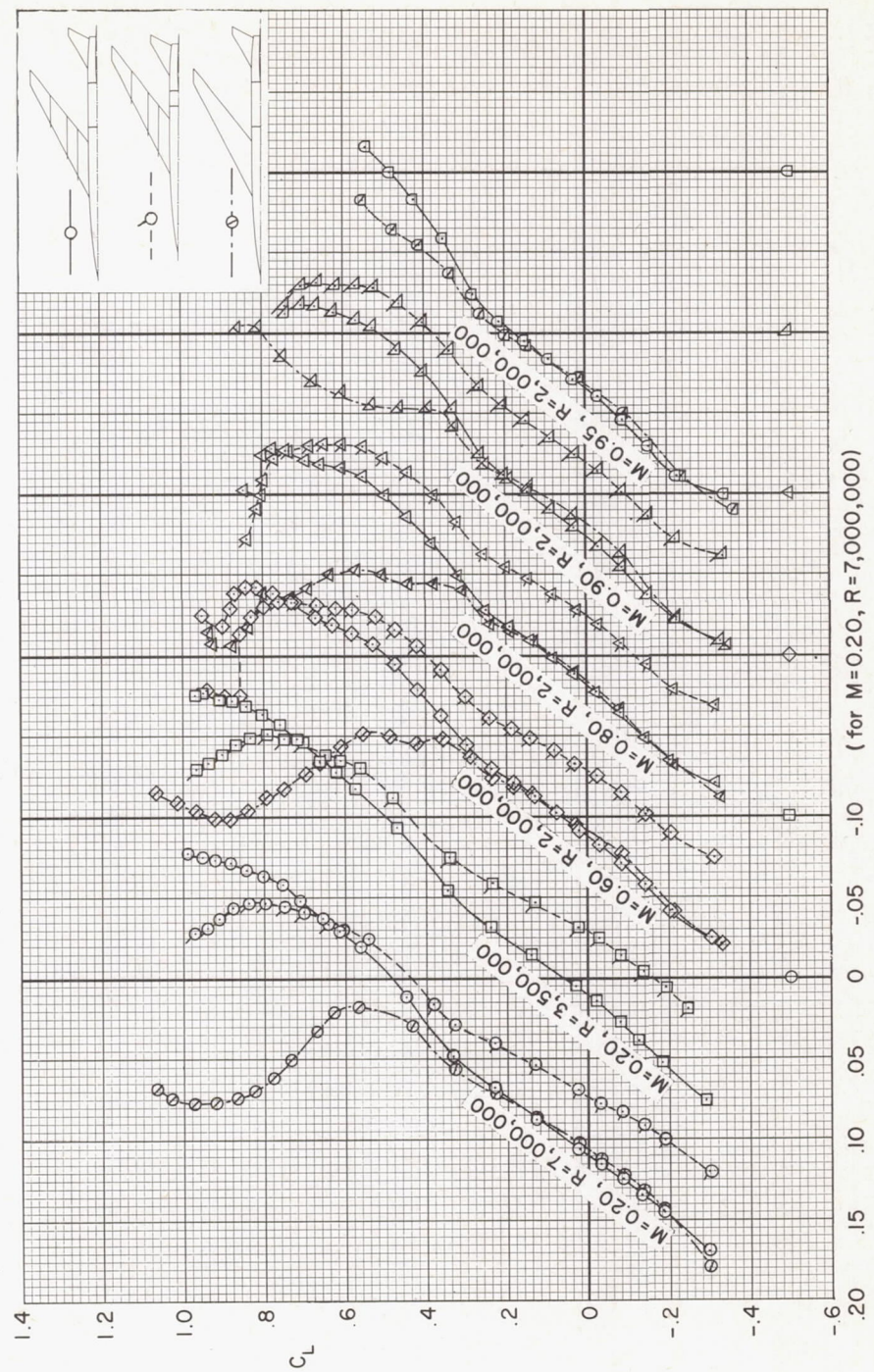
(b) $i_t = 0.2^\circ$

Figure 7.- Continued.



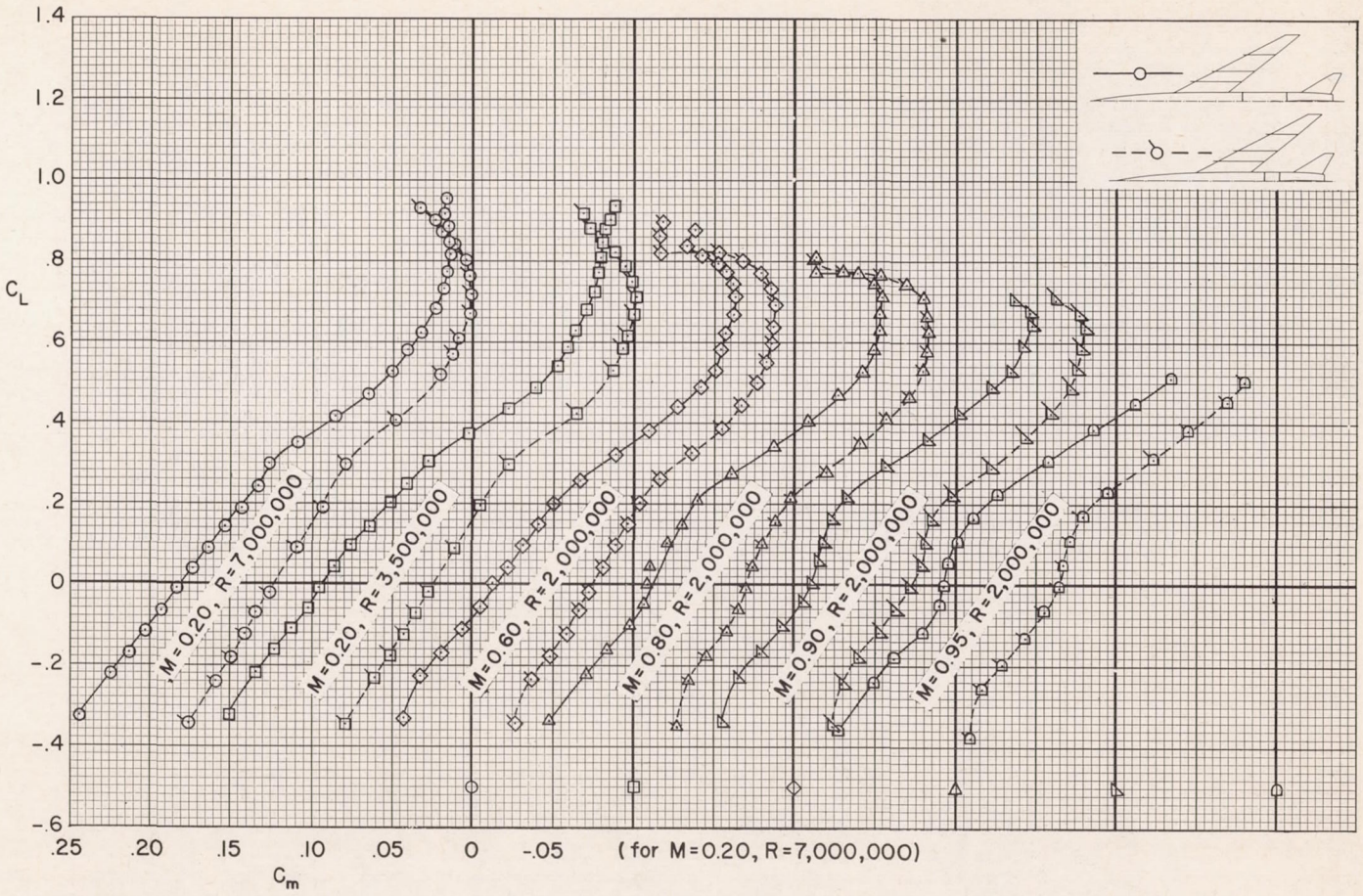
(c) $i_t = -3.9^\circ$

Figure 7.- Continued.



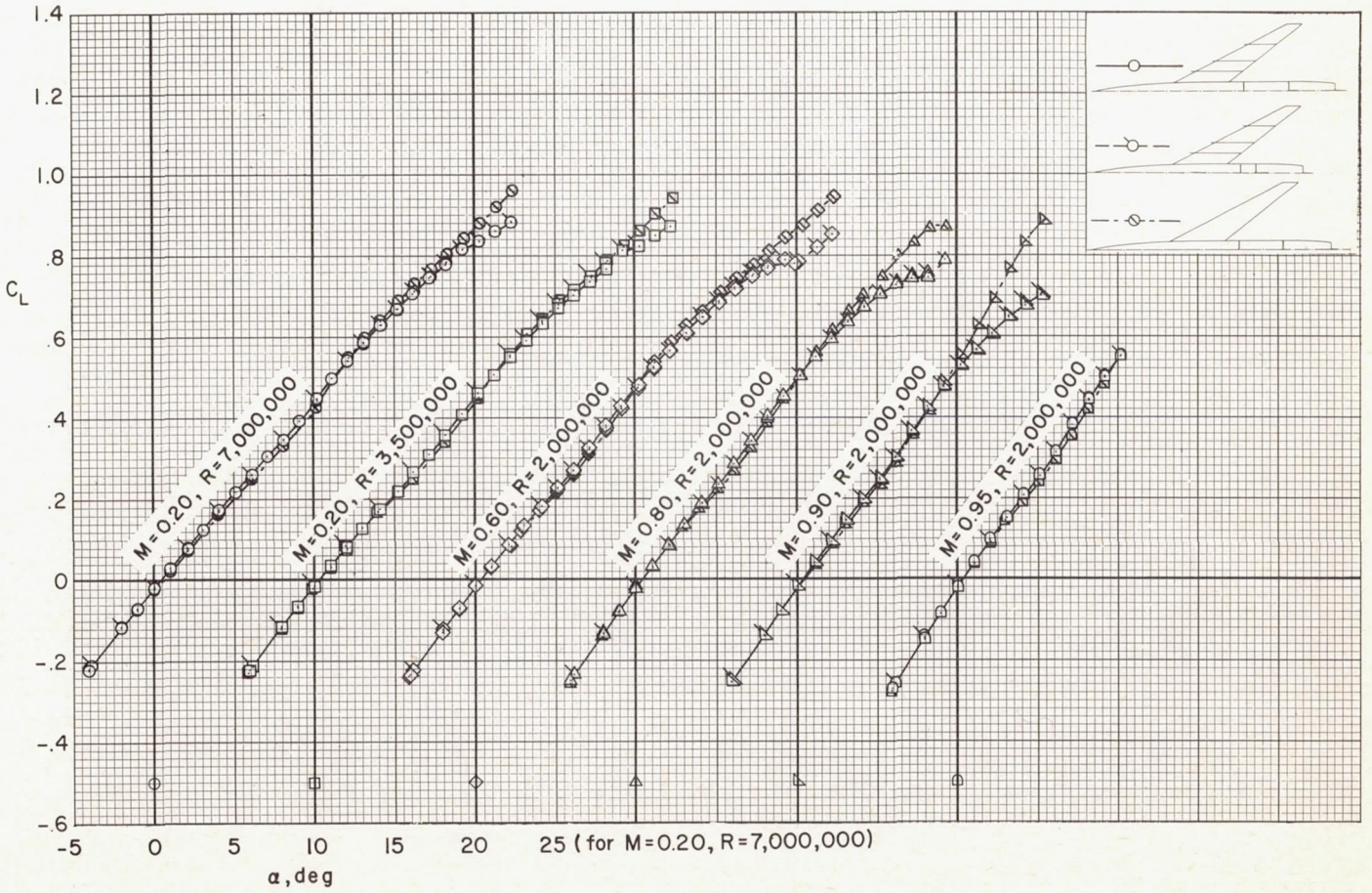
(d) $i_t = -7.8°$

Figure 7.- Continued.



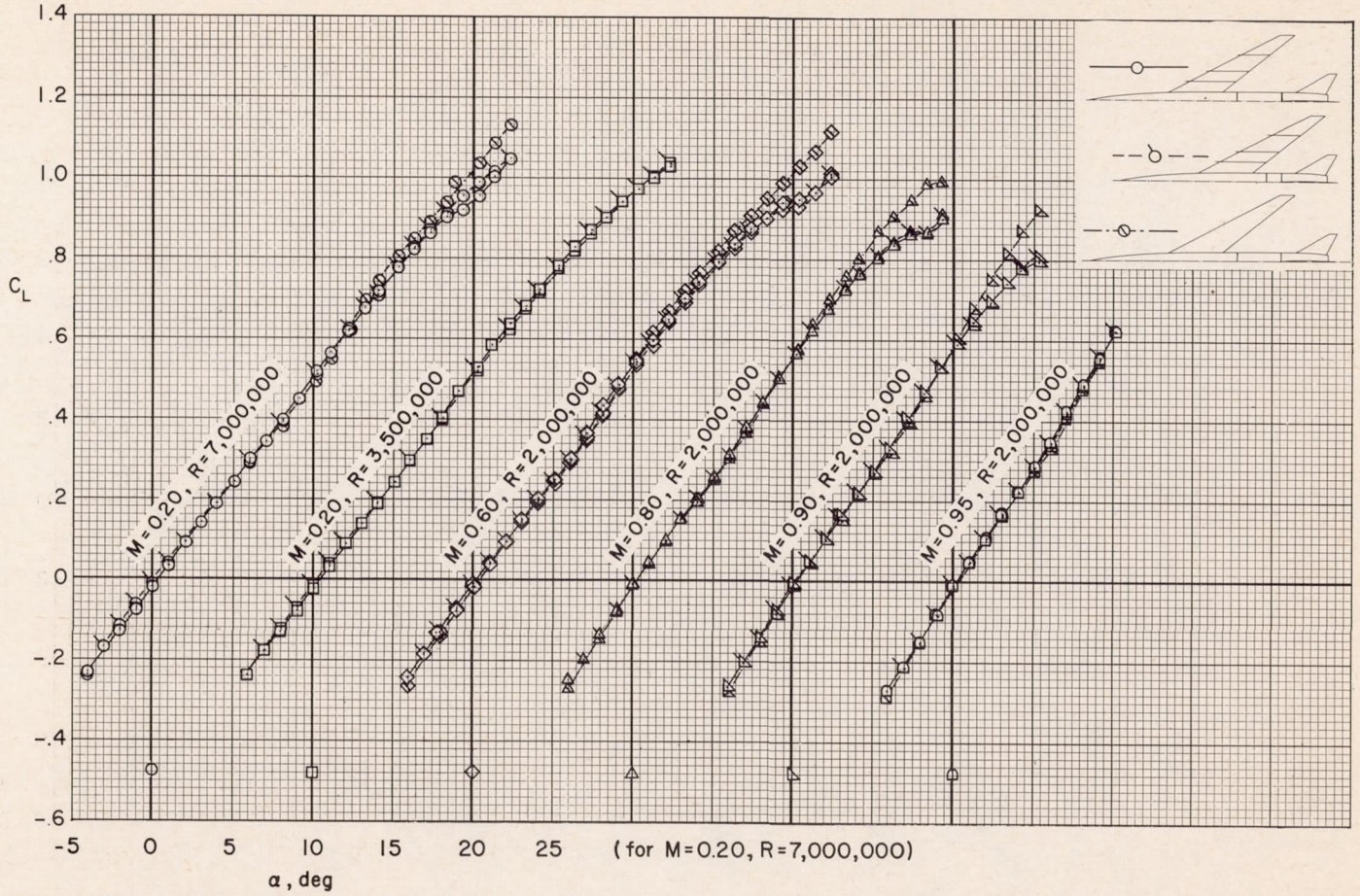
(e) $i_t = -11.7^\circ$

Figure 7.- Concluded.



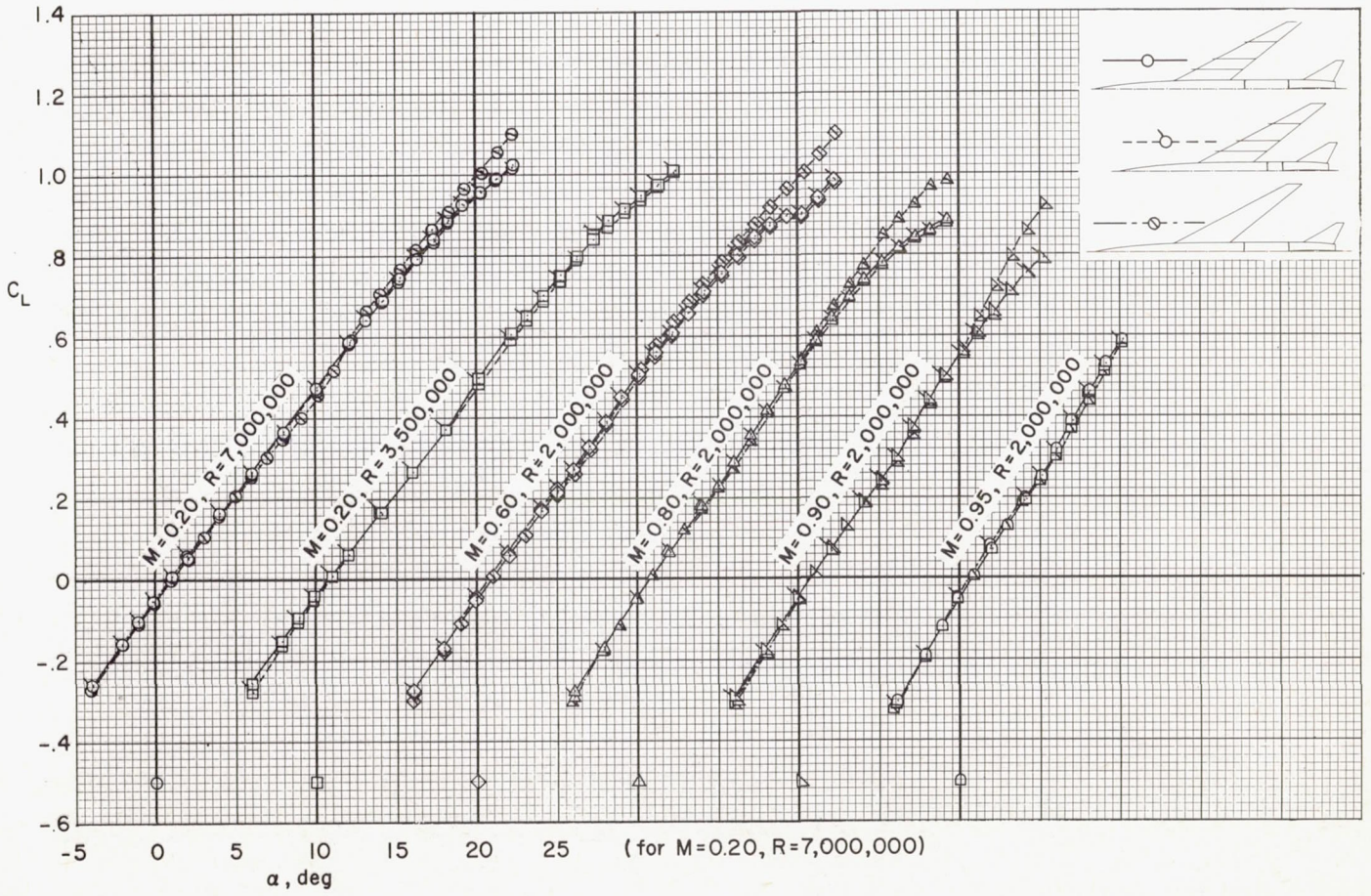
(a) Tail off.

Figure 8.- The lift characteristics of the model; wing in mid position, with and without fences (configuration X) and empennage (horizontal tail in mid position).



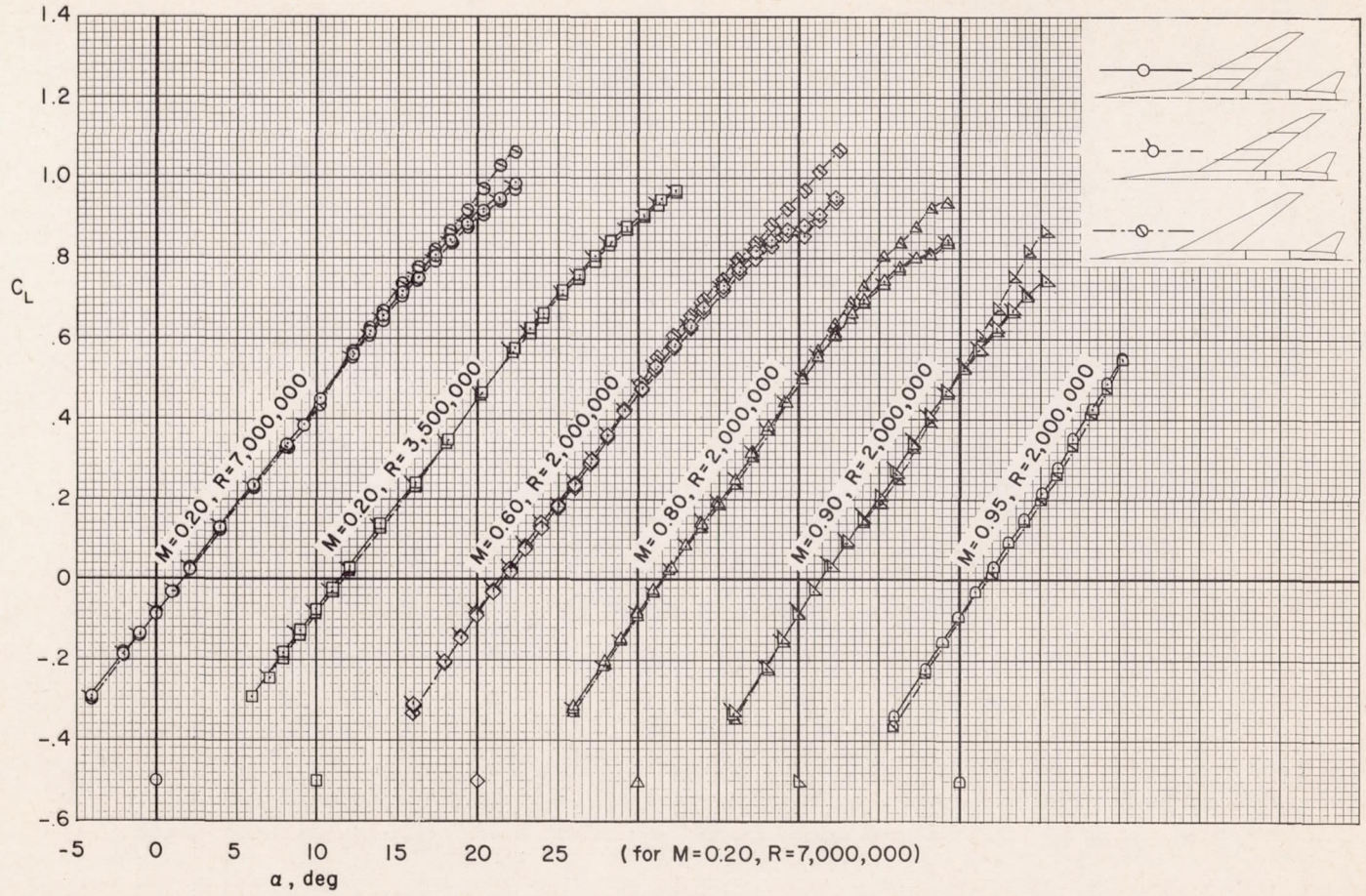
(b) $i_t = 0.2^\circ$

Figure 8.- Continued.



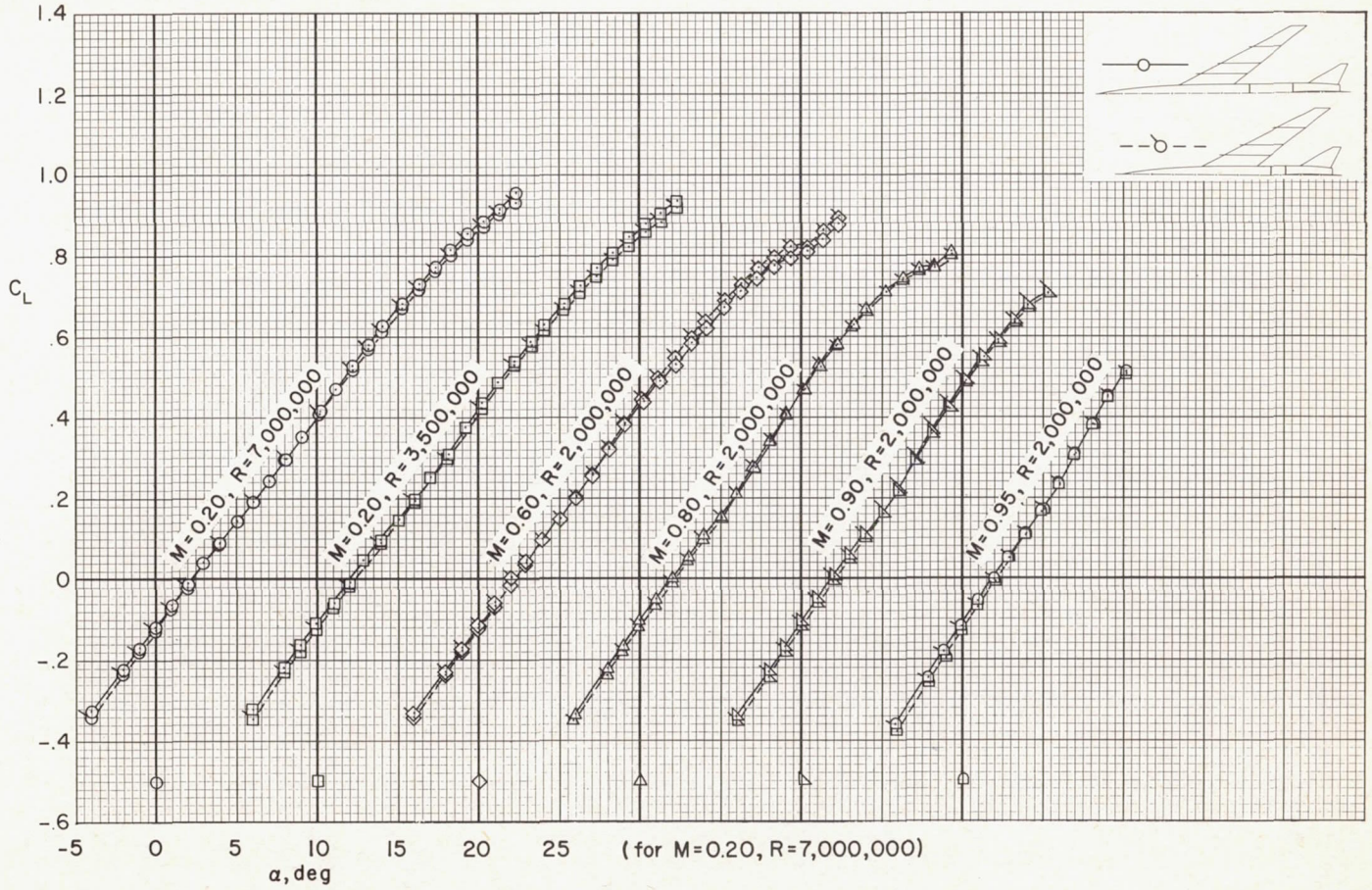
(c) $i_t = -3.9^\circ$

Figure 8.- Continued.



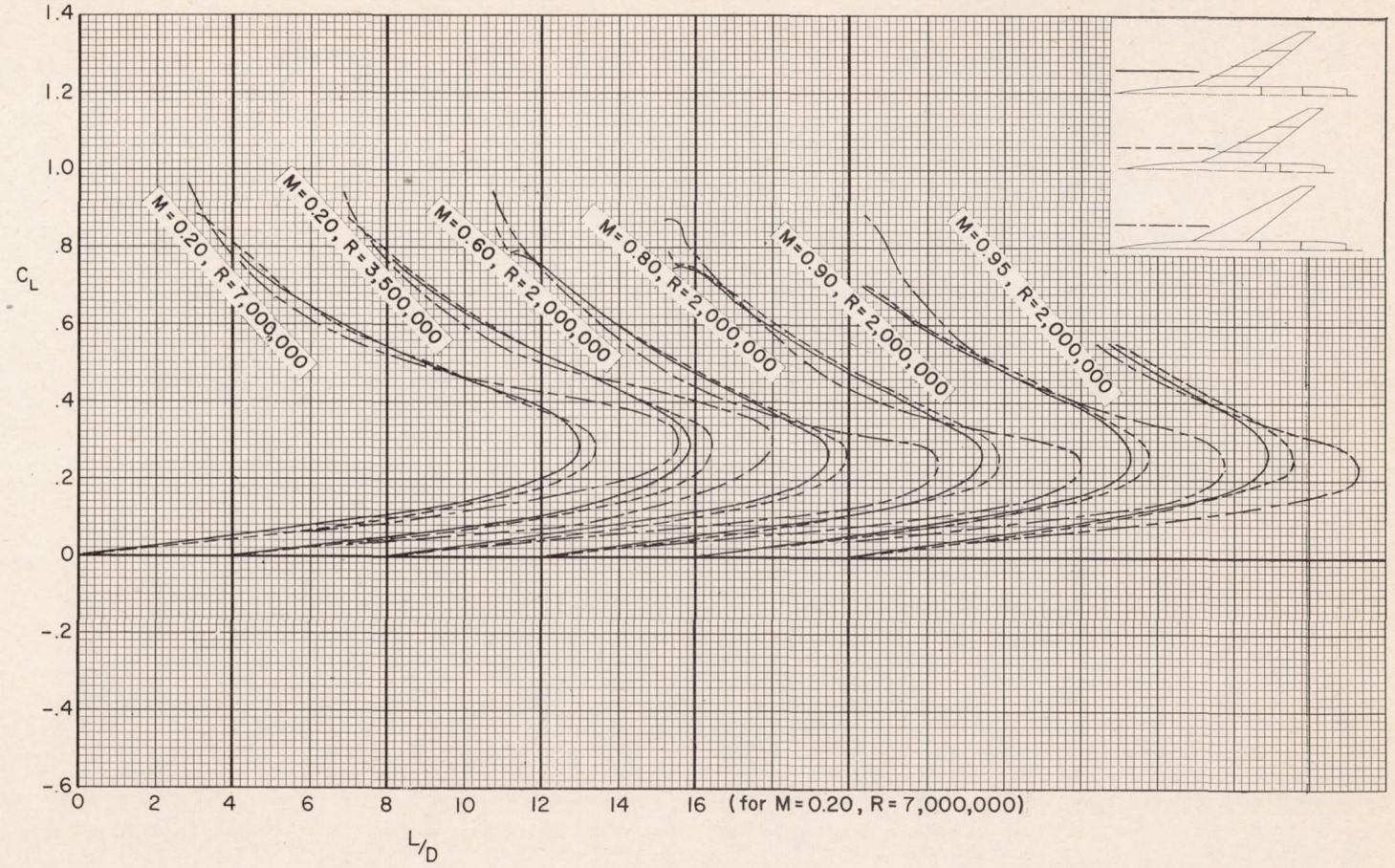
(d) $i_t = -7.8^\circ$

Figure 8.- Continued.



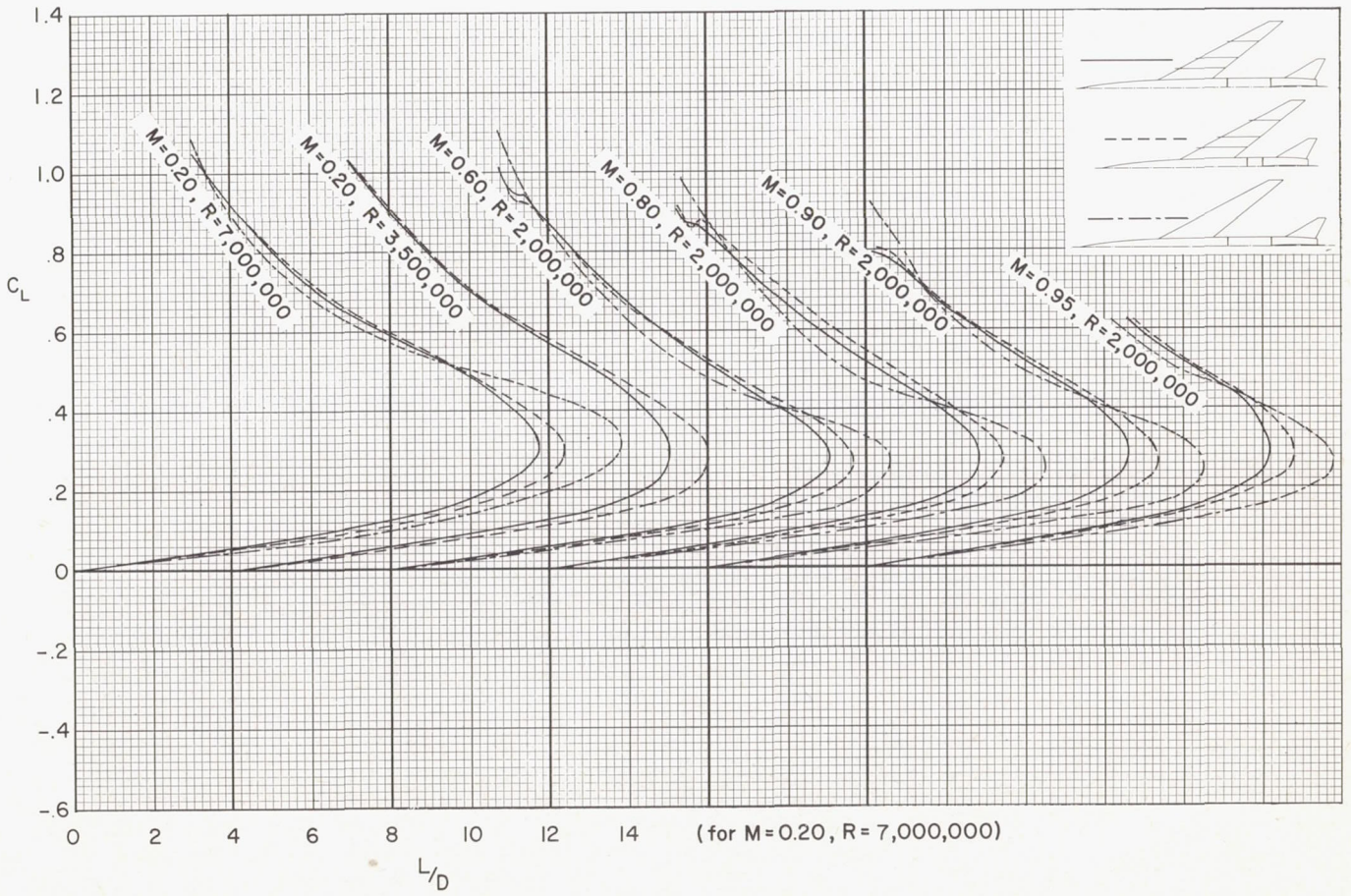
(e) $i_t = -11.7^\circ$

Figure 8.- Concluded.



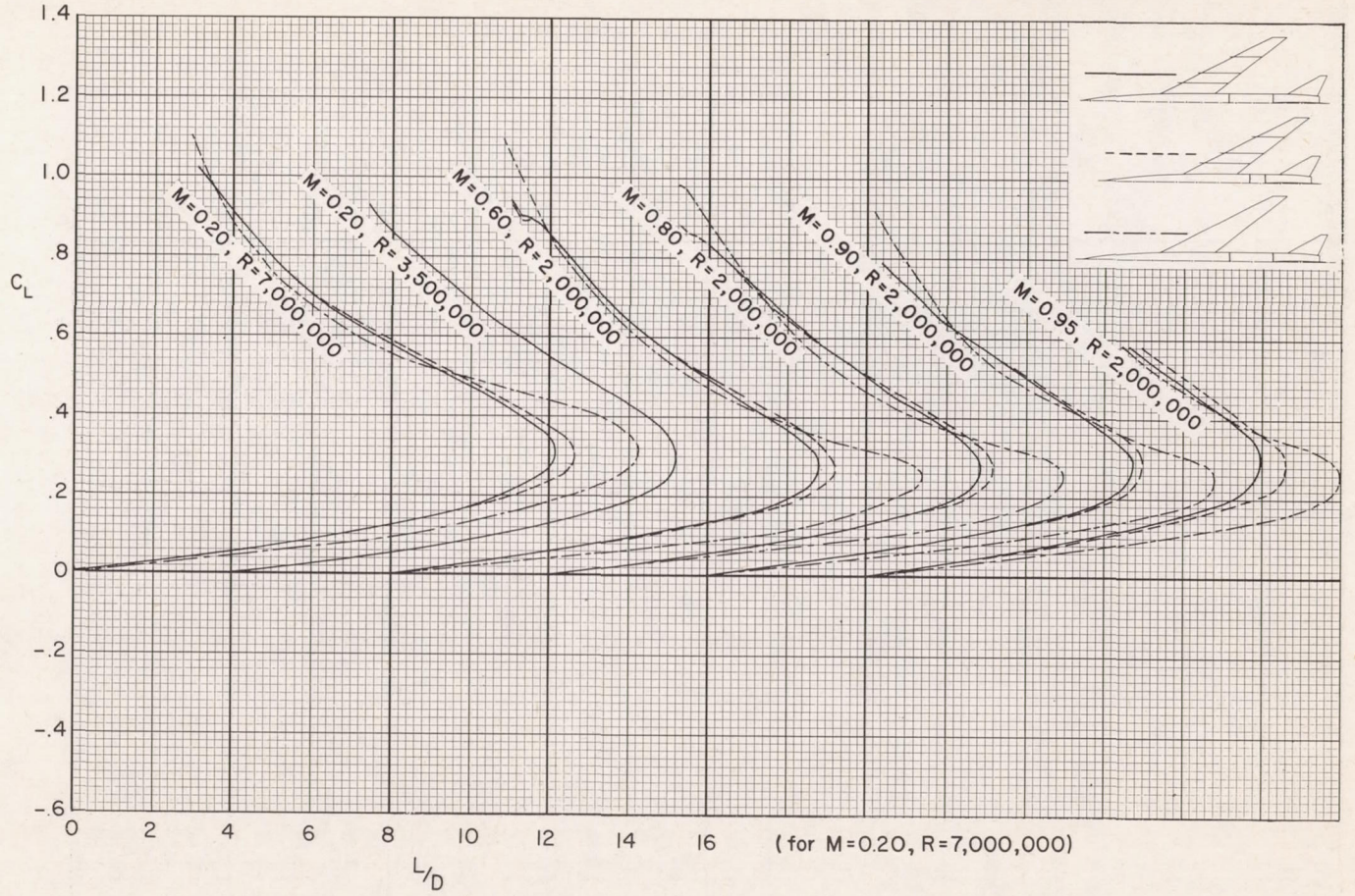
(a) Tail off.

Figure 9.- The lift-drag characteristics of the model; wing in mid position, with and without fences (configuration X) and empennage (horizontal tail in mid position).



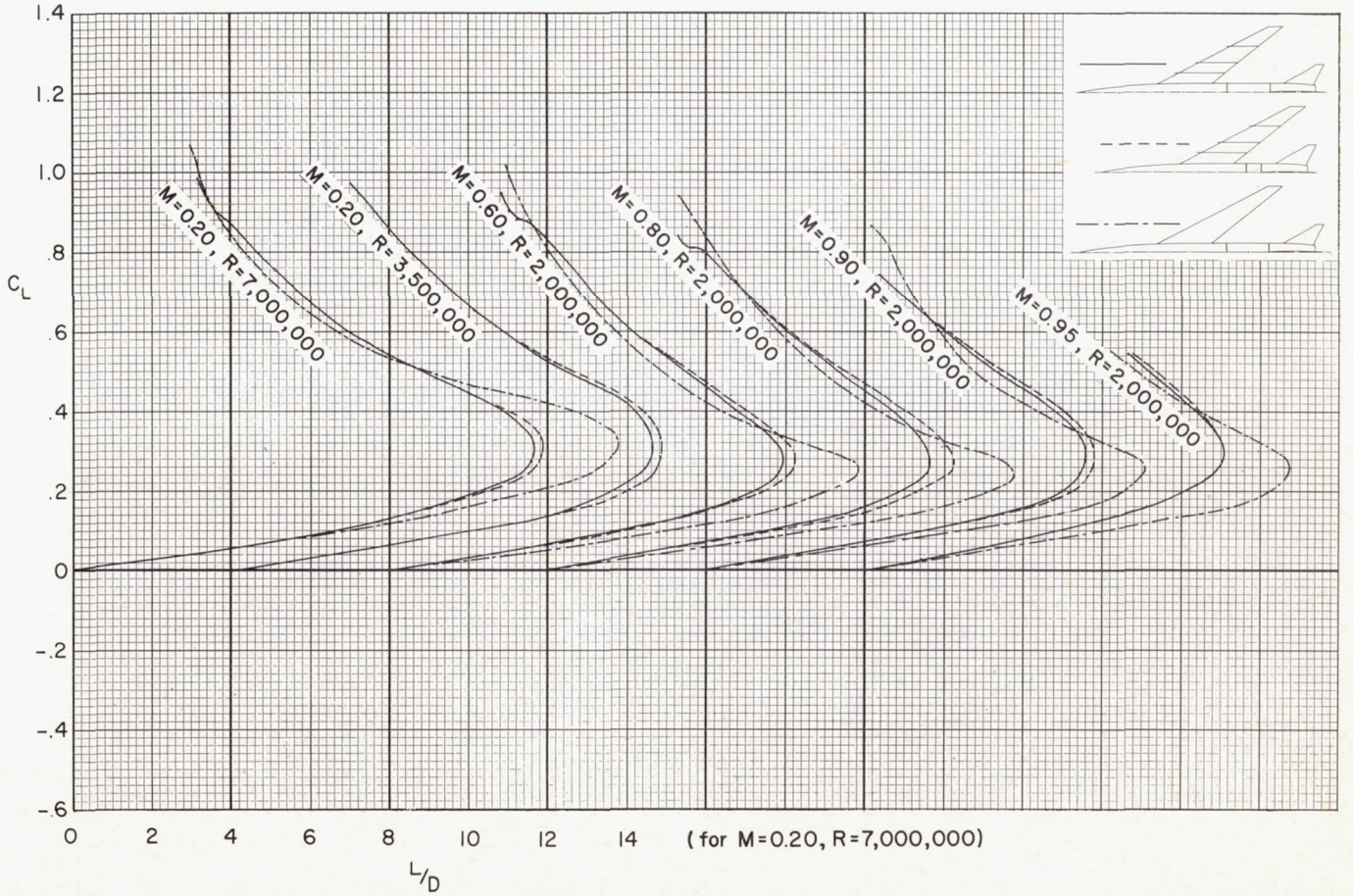
(b) $i_t = 0.2^\circ$

Figure 9.- Continued.



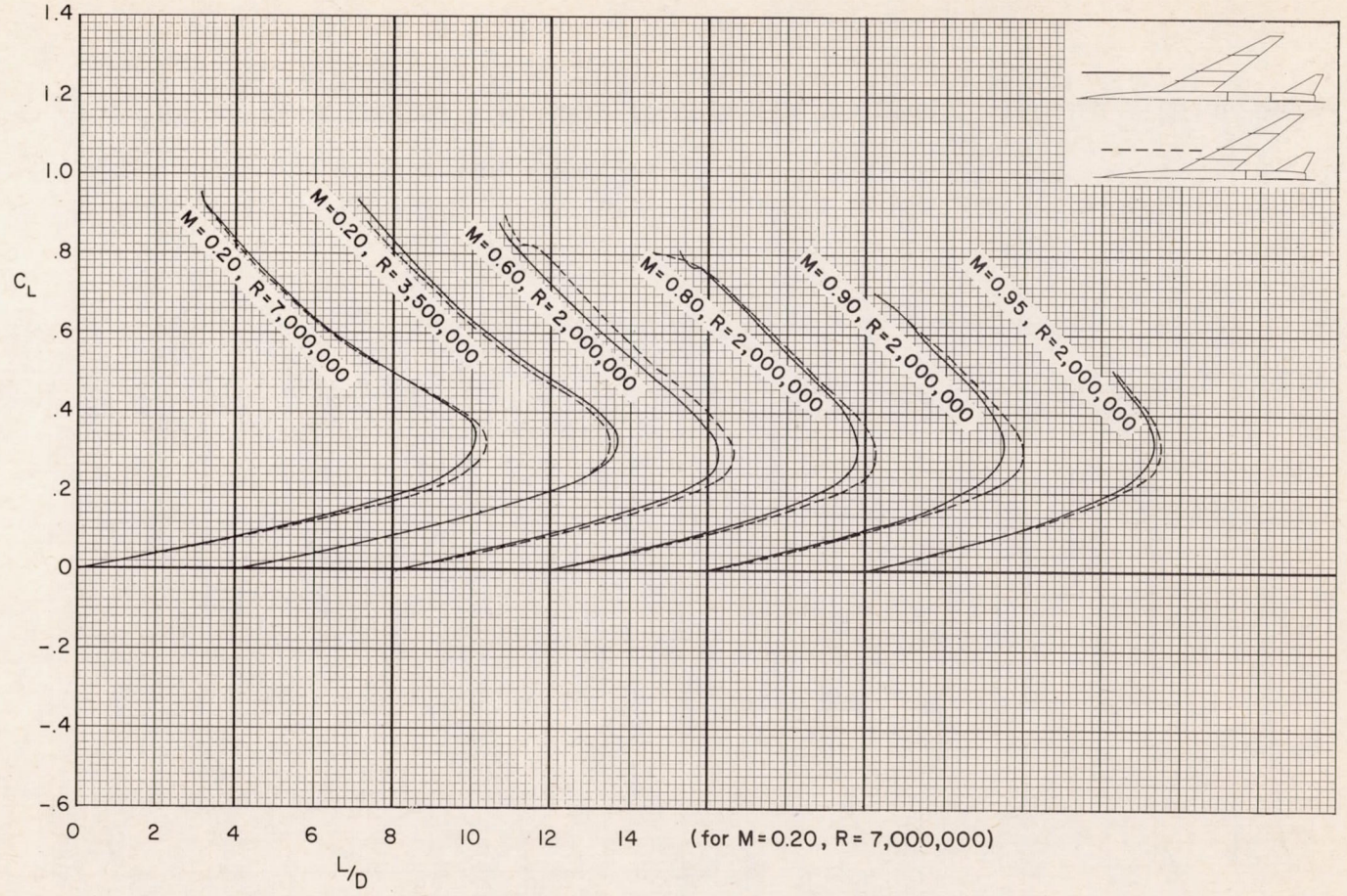
(c) $i_t = -3.9^\circ$

Figure 9.- Continued.



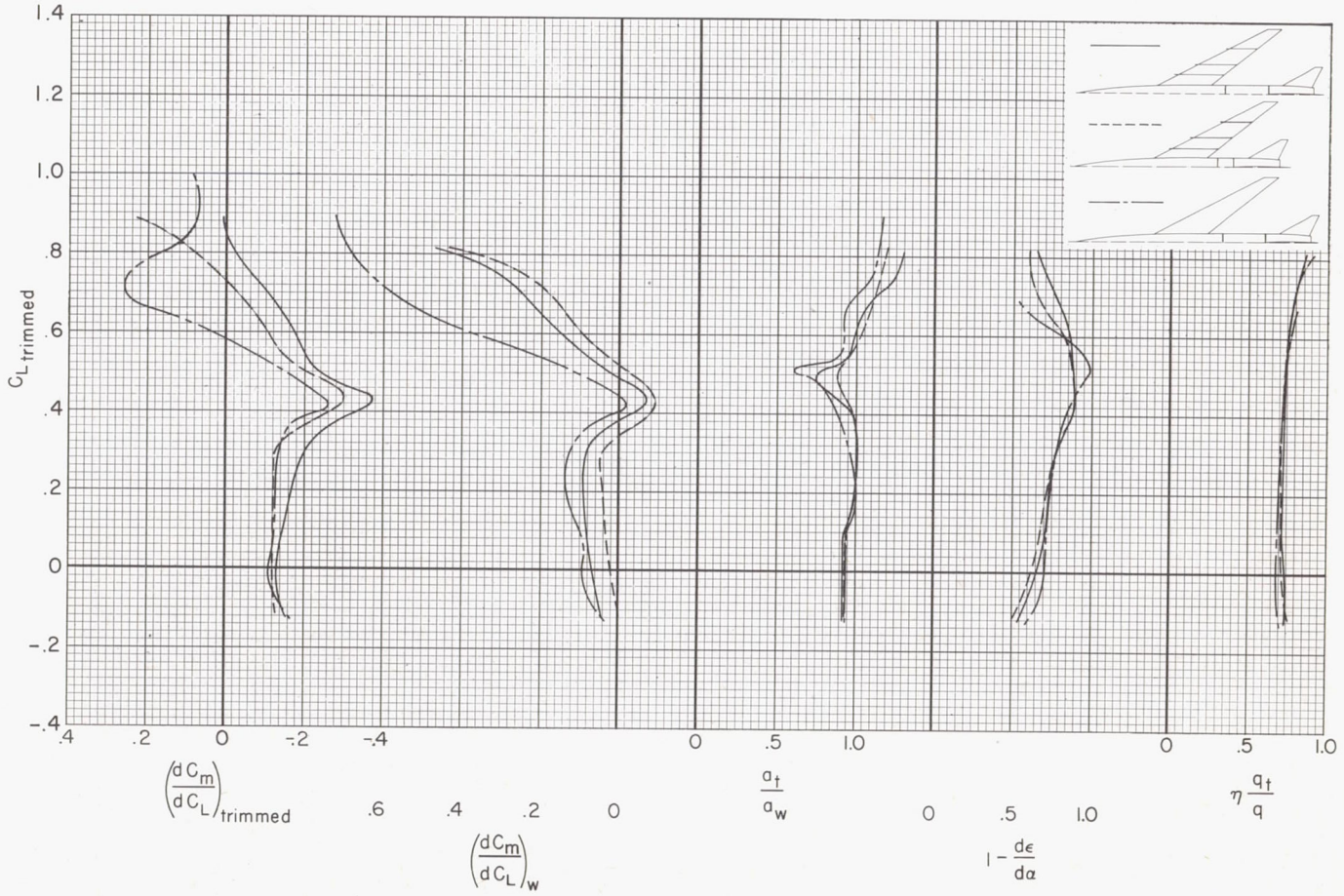
(d) $i_t = -7.8^\circ$

Figure 9.- Continued.



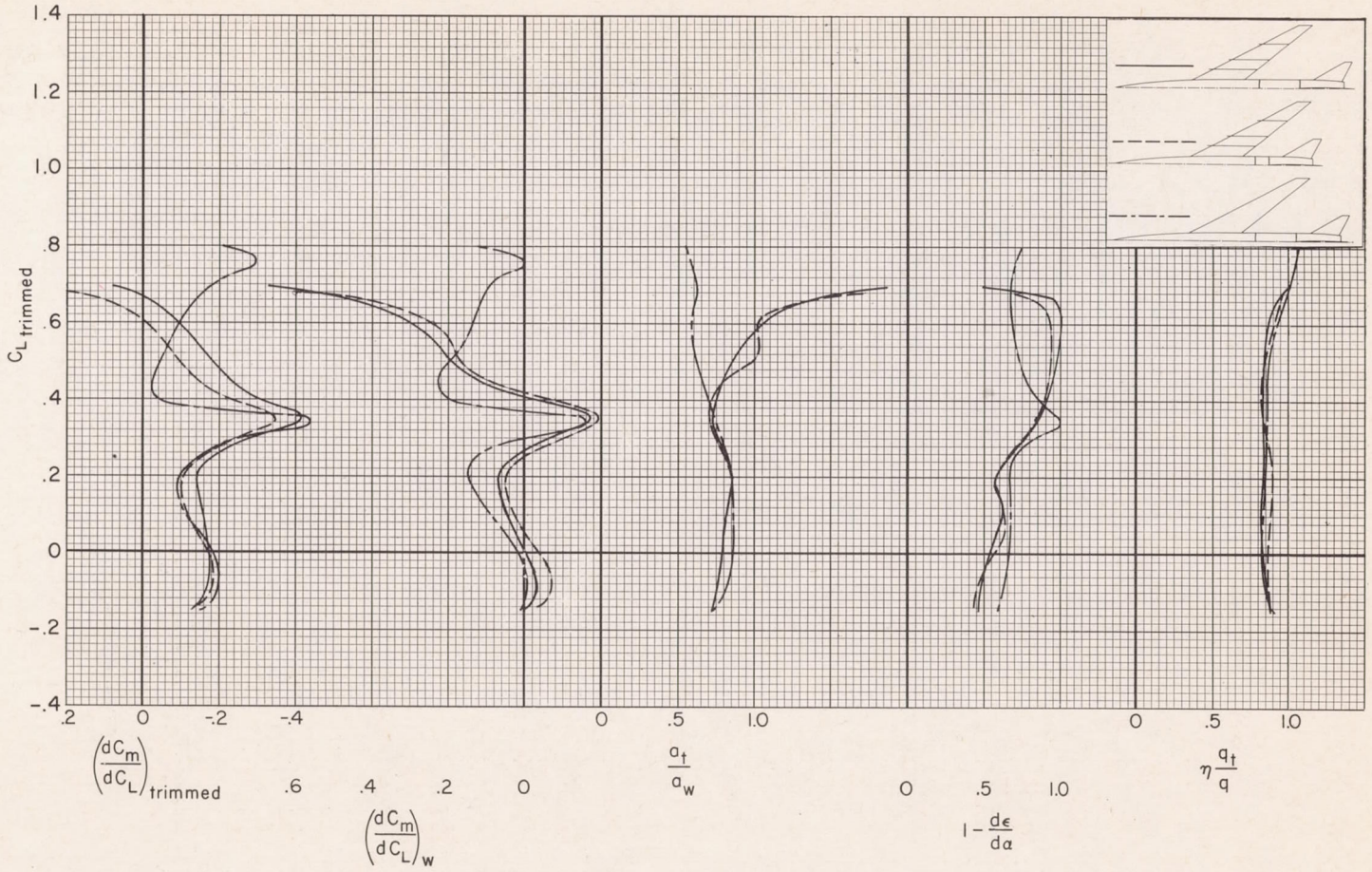
(e) $i_t = -11.7^\circ$

Figure 9.- Concluded.



(a) M = 0.20, R = 7,000,000

Figure 10.- Various longitudinal stability factors for the model; with and without fences (configuration X), wing and horizontal tail in mid position.



(b) M = 0.90, R = 2,000,000

Figure 10.- Concluded.

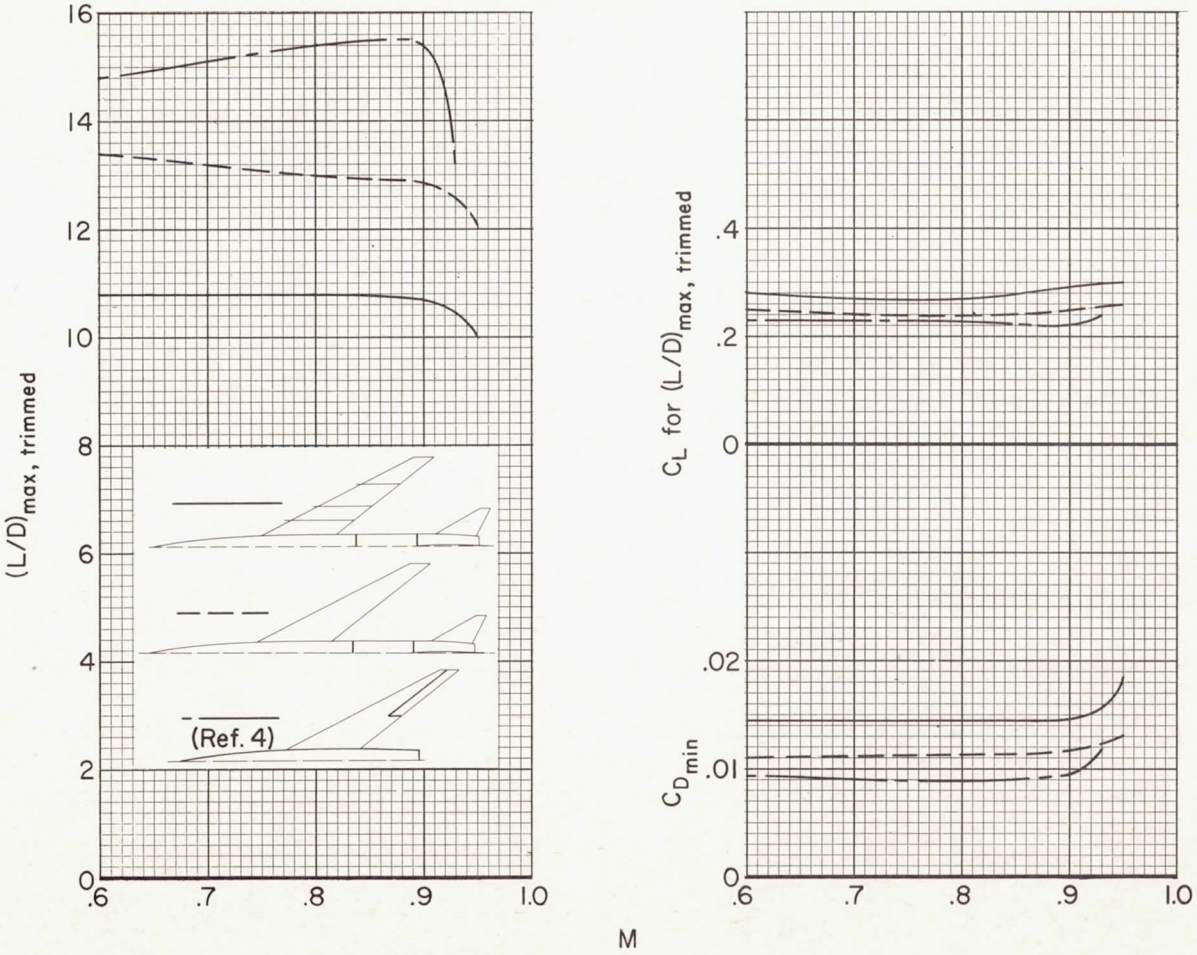


Figure 11.- A comparison of lift-drag and minimum-drag characteristics of the model when trimmed by a horizontal tail (mid-rear position) and by elevons (data of ref. 4). Tailed model with and without fences (configuration X), center of moments for data from reference 4 at 0.28 $\bar{c}$.